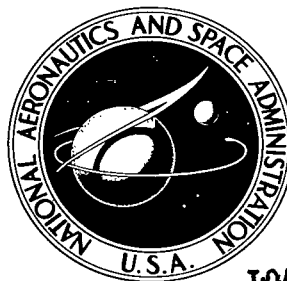


NASA TECHNICAL NOTE



NASA TN D-5981

e. 1

LOAN COPY: RETURN TO
AFWL (WLOL)
KIRTLAND AFB, N MEX



TECH LIBRARY KAFB, NM

NASA TN D-5981

A METHOD FOR COMPUTING EXTREMAL
MAXIMUM-RANGE THRUST-LIMITED
ROCKET TRAJECTORIES WITH
APPLICATION TO LUNAR TRANSPORT

*by A. Gary Childs, Ernest S. Armstrong,
and Athena T. Markos*

*Langley Research Center
Hampton, Va. 23365*



0132727

1. Report No. NASA TN D-5981	2. Government Accession No.	3. Recipient's Catalog No.	
4. Title and Subtitle A METHOD FOR COMPUTING EXTREMAL MAXIMUM-RANGE THRUST-LIMITED ROCKET TRAJECTORIES WITH APPLICATION TO LUNAR TRANSPORT	5. Report Date September 1970		6. Performing Organization Code
	7. Author(s) A. Gary Childs, Ernest S. Armstrong, and Athena T. Markos		8. Performing Organization Report No. L-7114
9. Performing Organization Name and Address NASA Langley Research Center Hampton, Va. 23365	10. Work Unit No. 125-19-08-04		11. Contract or Grant No.
	12. Sponsoring Agency Name and Address National Aeronautics and Space Administration Washington, D.C. 20546		13. Type of Report and Period Covered Technical Note
15. Supplementary Notes	14. Sponsoring Agency Code		
16. Abstract A technique is described for the effective computation of maximum range trajectories for a thrust-limited surface-to-surface rocket in a vacuum and a Keplerian gravity field. The technique is a combination of the Pontryagin maximum principle with an initial-value algorithm for the solution of two-point boundary-value problems developed by Armstrong. Application is made to lunar flight for a vehicle with an initial thrust-weight ratio of 5.0. Surface ranges obtained as a function of the percent of the vehicle weight used as fuel vary from only a few miles to almost one-half the moon's circumference.			
17. Key Words (Suggested by Author(s)) Optimal control theory Maximum range trajectories Nonlinear programing		18. Distribution Statement Unclassified - Unlimited	
19. Security Classif. (of this report) Unclassified	20. Security Classif. (of this page) Unclassified	21. No. of Pages 43	22. Price* \$3.00

A METHOD FOR COMPUTING EXTREMAL
MAXIMUM-RANGE THRUST-LIMITED ROCKET TRAJECTORIES
WITH APPLICATION TO LUNAR TRANSPORT

By A. Gary Childs, Ernest S. Armstrong,
and Athena T. Markos
Langley Research Center

SUMMARY

A computational technique has been described for the calculation of long-range extremal maximum-range thrust-limited trajectories for the transfer of a rocket vehicle between two points on the surface of an atmosphereless planet. The technique has been applied to compute such trajectories for the lunar surface with a vehicle having an initial lunar thrust-weight ratio of 5.0 for final to initial mass ratios from 0.95 to 0.326. General characteristics are given in graphical form and were observed from the results for all the mass ratios. The extremal trajectories and controls are given for the particular mass ratios, 0.65, 0.335, and 0.326. Parameters are presented which can be used (with a relatively simple computer program) to reconstruct completely optimal controls and trajectories for the mass ratios of this study with a thrust-weight ratio of 5.0.

INTRODUCTION

Extensive exploration of the lunar surface may require the use of rocket-propelled transportation vehicles. In order to design such vehicles and plan exploration missions, it is helpful to know the optimal relationships between fuel and range. These relationships are especially useful when long range flights are involved.

Manci (ref. 1) has considered the minimum fuel problem for fixed range and Childs and Armstrong (ref. 2) have considered the maximum range problem for fixed fuel. These studies involved thrust-limited rocket vehicles and assumed a uniform gravitational field and a soft landing. A soft landing is defined as one with near-zero velocity. Both studies have been applied to lunar flight. The results of these studies are valid if the resultant range is less than about 30 miles (48.28 km). For longer ranges both the curvature of the lunar surface and nonuniform gravitational field must be taken into account. Needham (ref. 3) has considered minimum-fuel thrust-limited trajectories with fixed range between points of launch and soft landing on a spherical moon with a Keplerian gravitational field.

The longest range reported is about 65 miles (104.6 km) for a rocket vehicle with an initial lunar thrust-weight ratio of 2.4. Computational difficulties precluded Needham obtaining solutions with longer ranges. Needham noted the desirability of an effective computational procedure to solve such problems.

The purpose of this paper is to demonstrate a highly effective computational procedure for obtaining optimal thrust-limited rocket trajectories in a vacuum and a Keplerian gravity field. This procedure combines the Pontryagin maximum principle of optimal control theory (ref. 4) with an initial-value algorithm for the solution of two-point boundary-value problems developed by Armstrong (ref. 5). Other applications of the procedure than those given in the present paper may be found in references 5, 6, and 7.

The dynamic equations for the present application are presented in nondimensional form. The trajectories are assumed to lie in a plane containing the center of gravitational attraction and the rocket launch position. The Pontryagin maximum principle is applied to obtain necessary conditions for maximal range with specified fuel. The application of the maximum principle leads to a two-point boundary-value problem which is solved by the initial-value algorithm. The procedure is exemplified by the lunar maximum-range—fixed-fuel flight of a rocket vehicle with an initial lunar thrust-weight ratio of 5. A family of extremal solutions with payload weight as parameter and the longest ranges about one-half the circumference of the moon is reported herein. Also, comparisons are made between the theoretical necessary conditions of the maximum principle for maximum range with fixed fuel and minimum fuel with fixed range and it is noted where the conditions coincide. The trajectories reported are shown to qualify as minimum-fuel solutions between their points of take-off and landing.

SYMBOLS

a_{ij}	elements of the matrix $\frac{\partial \vec{e}}{\partial \vec{\alpha}}$ ($i, j = 1, 2, 3$)
B	diagonal weighting matrix
b_i	elements of the matrix B ($i = 1, 2, 3$)
c	effective exhaust velocity
$E[\]$	scalar quantity measuring magnitude of \vec{e}
E	energy

\vec{e}	error vector
f_s	switching function (see eq. (8))
g	gravitational acceleration
H	Pontryagin pseudo-Hamiltonian (see eq. (4))
I_3	third-order identity matrix
i,j	indices
J	performance index
l	angular momentum
m	mass
p_i	Pontryagin auxiliary variables for maximum range problem ($i = 0, \dots, 5$)
r	radial polar coordinate
T	thrust
t	time
t_1, t_2	switching times
W_0	initial weight
W_f	final weight
$\vec{\alpha}$	parameter vector
α_i	elements of vector $\vec{\alpha}$ ($i = 1, 2, 3$)
γ	conditioning constant
$\delta\vec{\alpha}$	parameter correction vector

ϵ	eccentricity
θ	angular polar coordinate
λ_i	Pontryagin auxiliary variables for minimum fuel problem ($i = 0, 1, \dots, 5$)
μ	gravitational constant
ψ	control angle

Subscripts:

f	final
max	maximum
o	initial

Operations:

$(\bar{})$	() dimensionalized
$(\dot{})$	() differentiated with respect to time
$(\ddot{})$	() twice differentiated with respect to time
$\frac{\partial()}{\partial \vec{\alpha}}$	gradient of () in the direction of the vector $\vec{\alpha}$
$\frac{\partial()}{\partial \alpha_j}$	partial derivative of () with respect to α_j ($j = 1, 2, 3$)
$\text{diag}(,)$	matrix with diagonal elements (, ,)
$'$	matrix transpose
\equiv	identically equal
$(); []; []; ()$	intervals on the real line

ANALYSIS

Dynamic Equations

Figure 1 shows the coordinate system and force diagram for the problem. The equations of motion for two-dimensional motion above an atmosphereless spherical planet with an inverse-square-law gravitational field are

$$\left. \begin{aligned} \ddot{\bar{r}} &= \frac{\bar{T} \cos \psi}{\bar{m}} + \bar{r} \dot{\bar{\theta}}^2 - \frac{\bar{\mu}}{\bar{r}^2} \\ \ddot{\bar{\theta}} &= \frac{\bar{T} \sin \psi}{\bar{r} \bar{m}} - \frac{2\dot{\bar{r}} \dot{\bar{\theta}}}{\bar{r}} \\ \dot{\bar{m}} &= -\frac{\bar{T}}{\bar{c}} \end{aligned} \right\} \quad (1a)$$

where

- \bar{r}, θ polar coordinates
- \bar{T} thrust magnitude ($0 \leq \bar{T} \leq \bar{T}_{\max}$)
- ψ angle between thrust and radius
- \bar{m} vehicle mass
- \bar{c} rocket-engine effective exhaust speed
- $\bar{\mu}$ gravitational constant

Launch from rest, soft landing on the planetary surface, and maximized range give the following initial and terminal conditions:

$$\left. \begin{aligned} \bar{r}(\bar{t}_0) &= \bar{r}_0 & \bar{r}(\bar{t}_f) &= \bar{r}_0 \\ \dot{\bar{r}}(\bar{t}_0) &= 0 & \dot{\bar{r}}(\bar{t}_f) &= 0 \\ \theta(\bar{t}_0) &= 0 & \theta(\bar{t}_f) & \text{ maximized} \\ \dot{\bar{\theta}}(\bar{t}_0) &= 0 & \dot{\bar{\theta}}(\bar{t}_f) &= 0 \\ \bar{m}(\bar{t}_0) &= \bar{m}_0 & \bar{m}(\bar{t}_f) &= \bar{m}_f \end{aligned} \right\} \quad (1b)$$

where the subscripts o and f indicate the initial and final values of the variables. Equations (1a) and (1b) are nondimensionalized by use of the following relations:

$$\begin{aligned} r &= \frac{\bar{g}}{c^2} \bar{r} \\ t &= \frac{\bar{g}}{c} \bar{t} \\ m &= \frac{\bar{g}}{\bar{T}_{\max}} \bar{m} \\ T &= \frac{\bar{T}}{\bar{T}_{\max}} \\ \mu &= \frac{\bar{g}}{c^4} \bar{\mu} \end{aligned}$$

where the variables on the left are nondimensional, the surface gravitational acceleration is $\bar{g} = \frac{\bar{\mu}}{\bar{r}_0^2}$, and the maximum thrust capability of rocket engines is \bar{T}_{\max} . Nondimensional equations corresponding to equations (1a) are:

$$\left. \begin{aligned} \ddot{r} &= \frac{T \cos \psi}{m} + r\dot{\theta}^2 - \frac{\mu}{r^2} \\ \ddot{\theta} &= \frac{T \sin \psi}{rm} - \frac{2\dot{r}\dot{\theta}}{r} \\ \dot{m} &= -T \quad (0 \leq T \leq 1) \end{aligned} \right\} \quad (2)$$

The associated nondimensional initial and terminal conditions for equations (2) are given by equations (1b) without the bar notation.

Equations of Optimal Control

The Pontryagin maximum principle (ref. 4) is employed to obtain the equations for the optimal thrust magnitude and direction to maneuver the rocket from launch to a soft landing while $\theta(t_f)$ is maximized. Maximizing $\theta(t_f)$ is equivalent to minimizing the

Lagrangian performance index

$$J = \int_{t_0}^{t_f} -\dot{\theta} dt = -\theta(t_f) \quad (3)$$

The problem is mathematically much like the determination of Hamilton's canonical equations from Hamilton's principle for conservative systems. In the present case, however, the minimization of J is an optimization which is required in addition to the satisfaction of the principle and there are nonconservative forces involved. This additional optimization is possible because the control (a force) is left free to determine. The resulting equations, however, are canonically similar. The maximum principle as applied to the present problem states that in order for the integral J of equation (3) to be minimized, it is necessary that the following conditions be satisfied.

The controls T ($0 \leq T \leq 1$) and ψ must be chosen to maximize the so-called "Pontryagin pseudo-Hamiltonian" (mathematically analogous to the Hamiltonian of classical mechanics) which is given by

$$H = -p_0\dot{\theta} + p_1\dot{r} + p_2\left(r\dot{\theta}^2 + \frac{T \cos \psi}{m} - \frac{\mu}{r^2}\right) + p_3\dot{\theta} + p_4\left(\frac{T \sin \psi}{rm} - \frac{2\dot{r}\dot{\theta}}{r}\right) - p_5T \quad (4)$$

with the auxiliary variables (mathematically analogous to the conjugate momenta of classical mechanics) p_i ($i = 0, 1, \dots, 5$) satisfying

$$\left. \begin{aligned} p_0 &\leq 0 \\ \dot{p}_1 &= -p_2\dot{\theta}^2 - 2p_2\frac{\mu}{r^3} - 2p_4\frac{\dot{r}\dot{\theta}}{r^2} + \frac{Tp_4 \sin \psi}{mr^2} \\ \dot{p}_2 &= -p_1 + 2p_4\frac{\dot{\theta}}{r} \\ \dot{p}_3 &= 0 \\ \dot{p}_4 &= p_0 - 2p_2r\dot{\theta} - p_3 + 2p_4\frac{\dot{r}}{r} \\ \dot{p}_5 &= T \left[\frac{p_2 \cos \psi + p_4\left(\frac{\sin \psi}{r}\right)}{m^2} \right] \end{aligned} \right\} (p_3(t_f) = 0) \quad (5)$$

Also, when the end time t_f is not specified

$$H(t) \equiv 0 \quad (t_0 \leq t \leq t_f) \quad (6)$$

The controls as derived in reference 8 are given by

$$\left. \begin{aligned} T &= 1 & (f_s > 0) \\ T &= 0 & (f_s < 0) \end{aligned} \right\} \quad (7)$$

where the switching function for the rocket engine is

$$f_s = \frac{p_2 \cos \psi}{m} + \frac{p_4 \sin \psi}{rm} - p_5 \quad (8)$$

and, for $T \neq 0$,

$$\left. \begin{aligned} \cos \psi &= \frac{p_2}{\sqrt{p_2^2 + \left(\frac{p_4}{r}\right)^2}} \\ \sin \psi &= \frac{p_4}{r \sqrt{p_2^2 + \left(\frac{p_4}{r}\right)^2}} \end{aligned} \right\} \quad (9)$$

or

$$\tan \psi = \frac{p_4}{rp_2} \quad (10)$$

It is shown in reference 9 that trajectories occurring with $f_s(t) \equiv 0$ over a nonzero time interval in $[t_0, t_f]$ (singular trajectories) cannot be optimal for minimizing fuel. The same proof demonstrates that singular trajectories cannot be optimal for maximizing range. Such trajectories will therefore not be considered. The variable $p_5(t)$ for convenience may be eliminated from the problem and replaced by $f_s(t)$ as follows. Differentiating $f_s(t)$ given by equation (8) with respect to t and making use of equations (5) and (9) gives

$$\dot{f}_S = \frac{\frac{d}{dt} \left[\sqrt{p_2^2 + \left(\frac{p_4}{r}\right)^2} \right]}{m} \quad (11)$$

which is independent of p_5 .

Setting $H(t)$ to zero at $t = t_0$ and making use of the nondimensional initial conditions gives

$$T(t_0) f_S(t_0) - \frac{p_2(t_0) \mu}{r_0^2} = 0$$

It is assumed that $f_S(t_0) \geq 0$. If $f_S(t_0) = 0$, then $\frac{-p_2(t_0) \mu}{r_0^2} = 0$. If $f_S(t_0) > 0$, then from equation (7) $T(t_0) = 1$. In either case,

$$f_S(t_0) = \frac{p_2(t_0) \mu}{r_0^2} \quad (12)$$

The variable $p_5(t)$ may thus be eliminated and replaced by the differential equation (11) with initial condition (12)

Also abnormal ($p_0 = 0$) solutions (ref. 10, pp. 633-637) are not considered and for convenience p_0 is taken as -1.

From equations (7) it is seen that along a maximal range trajectory, the rocket burns with maximal burning rate $T = 1$ while $f_S > 0$, and coasts $T = 0$ along a Keplerian arc while $f_S < 0$. With t_0 interpreted as the launch time, the rocket burns with $T = 1$ from $t = t_0$ until such a time t_1 as f_S changes to a negative value. The rocket then coasts until such a time t_2 as f_S again becomes positive. This process continues until the first time t_f for which $m(t) = m_f$. Along the burning portions of the trajectory, the thrust direction is determined by equation (9) or (10). For the solutions presented, it was found that over a trajectory f_S changed sign twice and the trajectories could be characterized by initial ($t \in [t_0, t_1]$) and final ($t \in (t_2, t_f]$) burn periods separated by a single coast period ($t \in (t_1, t_2]$). Then t_f in terms of the specified initial and final mass and the two switching times is

$$t_f = m_0 - m_f + t_2 - t_1 \quad (13)$$

When the results are collected, it is seen that extremal maximum range trajectories satisfy the following set of simultaneous differential equations:

$$\left. \begin{aligned}
\ddot{r} &= \frac{Tp_2}{m\sqrt{p_2^2 + \left(\frac{p_4}{r}\right)^2}} + r\dot{\theta}^2 - \frac{\mu}{r^2} & \left(\begin{aligned} r(t_0) &= r(t_f) = r_0 \\ \dot{r}(t_0) &= \dot{r}(t_f) = 0 \end{aligned} \right) \\
\ddot{\theta} &= \frac{Tp_4}{mr^2\sqrt{p_2^2 + \left(\frac{p_4}{r}\right)^2}} - \frac{2\dot{r}\dot{\theta}}{r} & \left(\theta(t_0) = \dot{\theta}(t_0) = \dot{\theta}(t_f) = 0 \right) \\
\dot{m} &= -T & \left(\begin{aligned} m(t_0) &= m_0 \\ m(t_f) &= m_f \end{aligned} \right) \\
\dot{p}_1 &= -p_2\dot{\theta}^2 - 2p_2\frac{\mu}{r^3} - 2p_4\frac{\dot{r}\dot{\theta}}{r^2} + \frac{Tp_4^2}{mr^3\sqrt{p_2^2 + \left(\frac{p_4}{r}\right)^2}} \\
\dot{p}_2 &= -p_1 + 2p_4\frac{\dot{\theta}}{r} \\
\dot{p}_4 &= -1 - 2p_2r\dot{\theta} + 2p_4\frac{\dot{r}}{r} \\
\dot{f}_S &= \frac{\frac{d}{dt}\sqrt{p_2^2 + \left(\frac{p_4}{r}\right)^2}}{m} & \left(f_S(t_0) = \frac{p_2(t_0)\mu}{r_0^2} \right)
\end{aligned} \right\} \quad (14)$$

where

$$T = 1 \quad (f_S > 0)$$

$$T = 0 \quad (f_S < 0)$$

In order to solve these equations, it is necessary to solve numerically a two-point boundary-value problem.

With the following parameters given:

$$r(t_0) = r_0$$

$$\dot{r}(t_0) = 0$$

$$\theta(t_0) = 0$$

$$\dot{\theta}(t_0) = 0$$

$$m(t_0) = m_0$$

find $p_1(t_0)$, $p_2(t_0)$, and $p_4(t_0)$ so that at t_f

$$r(t_f) = r_0$$

$$\dot{r}(t_f) = 0$$

$$\dot{\theta}(t_f) = 0$$

$$m(t_f) = m_f$$

The method used to solve this boundary-value problem is that discussed in reference 5 and outlined in appendix A. The general solution of the boundary-value problem given by equations (14) has been programed for the Control Data 6600 electronic data processing system with the Fortran IV language. The program represents a useful computational procedure for the study of the class of thrust-limited maximum-range problems considered in this paper. A copy of the computer program is available from the authors upon request. A typical family of solutions for the lunar surface is presented in the next section.

RESULTS

Extremal maximal range results are presented for a rocket vehicle with an effective exhaust speed, initial mass, and maximal thrust capability of

$$\bar{c} = 9853.2 \text{ ft/sec} \quad (3003.3 \text{ m/sec})$$

$$\bar{m}_0 = 132 \text{ slugs} \quad (1926 \text{ kg})$$

$$\bar{T}_{\max} = 3503.8 \text{ lb} \quad (15\,585.7 \text{ N})$$

Taking the lunar surface acceleration due to gravity as

$$\bar{g} = 5.316 \text{ ft/sec}^2 \quad (1.620 \text{ m/sec}^2)$$

gives an initial thrust-weight ratio of

$$\frac{\bar{T}_{\max}}{\bar{m}_0 \bar{g}} = 5 = \frac{1}{\bar{m}_0}$$

or

$$\bar{m}_0 = 0.2$$

The value of \bar{r}_0 was taken as $5.702 \times 10^6 \text{ ft}$ ($1.738 \times 10^6 \text{ m}$).

Solutions were found for a set of values of m_f/m_0 ($= \bar{m}_f/\bar{m}_0$) obtained by fixing m_0 at 0.2 and varying m_f so that m_f/m_0 ranged from 0.95 to 0.326 in steps sufficiently small to assure convergence of the iterative procedure (see appendix A) used in solving equations (14). Each solution was found to have initial and final maximal thrust periods over the time intervals $[\bar{t}_0, \bar{t}_1]$ and $(\bar{t}_2, \bar{t}_f]$, respectively, separated by a coast period over $(\bar{t}_1, \bar{t}_2]$. Results needed to reconstruct the trajectories are given in table I. Solutions were not obtained below $m_f/m_0 = 0.326$ because of convergence difficulties in the iterative procedure. Past this point the terminal values of \bar{r} , $\dot{\bar{r}}$, and $\dot{\bar{\theta}}$ became sufficiently insensitive to changes in the $p_i(t_0)$ ($i = 1, 2, 4$) to lower the convergence rate to a point where the acquisition of additional solutions was too expensive in terms of computer time. This difficulty is reflected by the sharp increase in the values of the auxiliary variables at $m_f/m_0 = 0.326$.

TABLE I. - CHARACTERISTICS OF EXTREMAL MAXIMUM RANGE SOLUTIONS

Mass ratio	Initial values of auxiliary variables, nondimensional			Switching and final times, sec			Range, miles (km)
m_f/m_0	$p_1(t_0)$	$p_2(t_0)$	$p_4(t_0)$	\bar{t}_1	\bar{t}_2	\bar{t}_f	$\bar{r}_0 \theta(\bar{t}_f)$
0.95	0.01096	0.05603	0.01884	9.414	60.48	69.62	1.973 (3.175)
.89	.03552	.1288	.04323	21.08	138.9	158.6	10.27 (16.53)
.83	.07606	.2096	.07041	33.19	225.3	255.3	26.59 (42.79)
.75	.1647	.3355	.1134	50.07	357.7	400.4	64.96 (104.5)
.65	.3683	.5433	.1873	72.71	566.6	624.0	153.8 (247.5)
.55	.7797	.8569	.3096	96.92	856.9	927.0	321.1 (516.8)
.45	1.814	1.455	.5923	123.5	1329	1415	670.6 (1079)
.40	3.178	2.072	.9712	138.0	1738	1827	1024 (1648)
.38	4.170	2.448	1.256	143.6	1954	2041	1229 (1978)
.37	4.932	2.706	1.481	146.6	2085	2172	1365 (2197)
.36	6.000	3.034	1.802	149.7	2233	2321	1530 (2462)
.35	7.650	3.478	2.311	152.7	2404	2493	1738 (2797)
.335	13.81	4.758	4.278	157.2	2723	2813	2216 (3566)
^a .326	74.94	13.49	24.51	159.7	3000	3090	2938 (4728)

^aNegative altitude during early part of trajectory.

In all cases convergence was obtained to within $\pm 10^{-3}$ feet (3×10^{-4} m) of $\bar{r}(\bar{t}_f) = \bar{r}_0, \pm 0.1$ ft/sec (0.03 m/sec) of $\dot{\bar{r}}(\bar{t}_f) = 0$, and $\pm 10^{-6}$ rad/sec of $\dot{\bar{\theta}}(\bar{t}_f) = 0$.

For each solution, $p_5(\bar{t}_f) > 0$ whereby it is also a minimum fuel extremal. (See appendix B.)

Figure 2 gives lunar surface range $\bar{r}_0 \theta(\bar{t}_f)$ as a function of final to initial mass ratio \bar{m}_f/\bar{m}_0 . Surface range appears to increase exponentially for decreasing payload \bar{m}_f and thus indicates that for larger amounts of fuel, the extremal trajectories deliver many more units of range per unit mass of fuel.

As can be seen from table I, the duration of the coast periods increases for decreasing payload varying from about 74 percent of the total flight time for $m_f/m_0 = 0.95$ to about 92 percent for $m_f/m_0 = 0.326$. For all values of m_f/m_0 , the range accrued over the coast period was found to be the predominant part of the total range and, overall, the range accrued over the coast periods increased with increasing fuel. The percentage of fuel used for injection into the coast phase increased with increasing fuel supply and ranged from 3.7 percent ($m_f/m_0 = 0.95$) to 43 percent ($m_f/m_0 = 0.326$).

For all m_f/m_0 the coast orbits were elliptic and became nearly parabolic for $m_f/m_0 = 0.95$. Figure 3 shows the coast phase eccentricity as a function of m_f/m_0 . The trajectories displayed increasing coast energy and angular momentum for increasing fuel supply. Maximal radial distances on the trajectories occurred during the coast periods. Maximal altitude $\bar{r}_{\max} - \bar{r}_0$ as a function of surface range $\bar{r}_0 \theta(\bar{t}_f)$ is shown in figure 4. The points of maximal radial distance are also the points of minimal $\bar{\theta}$. Figure 5 shows that the minimal $\bar{\theta}$ at the peak altitudes on the coast orbits increases with fuel supply. The behavior of $\bar{r}_{\max} - \bar{r}_0$ in figure 4 may be explained by recalling that over the coast periods,

$$\bar{\theta} = \frac{\bar{l}}{\bar{m} \bar{r}^2}$$

and noting that, for given angular momentum \bar{l} and mass \bar{m} , minimal $\bar{\theta}$ may be increased by decreasing \bar{r}_{\max} . However, the case of a low orbit is tempered by the fact that lower orbits possess higher kinetic energy which must be dissipated to make a soft landing. Thus, lowering the orbit is postponed until the payload is sufficiently small to give a large deceleration capacity for soft landing.

Figure 6 presents detailed results for $\bar{m}_f/\bar{m}_0 = 0.65$. Figure 6(a) gives the thrust angle ψ over the launch and landing phases. The angle ψ is undefined over the coast phase. Figure 6(b) gives altitude $\bar{r} - \bar{r}_0$ as a function of range $\bar{r}_0 \theta(\bar{t})$. Figure 6(c)

gives altitude as a function of flight time. Figures 6(d) and 6(e) give radial $\dot{\bar{r}}$ and tangential $\dot{\bar{r}}\bar{\theta}$ velocity time histories. Figure 7 gives similar results for $\bar{m}_f/\bar{m}_0 = 0.335$.

The general characteristics given in figure 6 for m_f/m_0 are typical of the intermediate range solutions. Results for a typical long-range solution $m_f/m_0 = 0.335$ are given in figure 7. Figure 8 presents results for $m_f/m_0 = 0.326$, the smallest ratio for which a solution was obtained. For this case a dip beneath the lunar surface is noted during the initial thrusting phase. Such dips will always occur when the initial angle $90^\circ - \psi$ is less than $11^\circ 32' = \sin^{-1} \frac{\bar{m}_0 g}{T_{\max}}$ and causes the radial component of thrust to be less than the gravitational force.

From figure 3 it appears that for some value of m_f/m_0 less than 0.326 (approximately 0.320 by extrapolation), the coast trajectory will become circular. Figure 9 shows coast orbit eccentricity as a function of maximal altitude. This curve is not as easily extrapolated as that of figure 3 to estimate the altitude of the circular orbit. However, the specific energy (energy per unit mass) of the coast orbits is monotonically increasing for decreasing m_f/m_0 with $E/m = -1.5291 \times 10^7 \text{ ft}^2/\text{sec}^4$ ($-0.1421 \times 10^7 \text{ m}^2/\text{sec}^4$) for $m_f/m_0 = 0.326$ and $E/m = -\frac{\mu}{2r_0} = -1.5154 \times 10^7 \text{ ft}^2/\text{sec}^4$ ($-0.1408 \times 10^7 \text{ m}^2/\text{sec}^4$) for a circular orbit about the lunar surface. It is thus conjectured that the circular orbit will have near-zero altitude. Since no altitude constraints have been theoretically imposed, the thrusting part of this trajectory may contain negative altitudes as did the $m_f/m_0 = 0.326$ case.

If it is recalled that the range accrued over the coast phase was, in all solutions obtained, the predominant part of the total range, it is evident that the most important characteristic of each extremal is the coast phase. This result should follow for other lunar rocket vehicles as well as for the one considered herein. Although, in practice, it may not be possible to follow exactly an extremal trajectory for a given vehicle and value of m_f/m_0 , an attempt could be made to achieve the corresponding coast phase as efficiently as possible. In this way near theoretical extremal range should be obtained.

Solutions for rocket-engine configurations different from the one considered herein may be similarly obtained by the computational procedure presented.

CONCLUDING REMARKS

A program for obtaining maximum-range thrust-limited rocket trajectories between points of launch and soft landing on the surface of an atmosphereless planet has been described. An application of the program for the lunar surface has produced trajectories

for a vehicle with a lunar thrust-weight ratio of 5.0. Results are presented for final to initial mass ratios from 0.95 to 0.326, the longest trajectory being about 3000 miles (4827.9 km). The trajectories presented were shown in an appendix to qualify as minimum fuel extremals between the points of launch and soft landing.

Since the primary purpose of this paper is the demonstration of the capability of calculating long maximum range trajectories in a Keplerian gravitational field, results have only been obtained and presented for one value of lunar thrust-weight ratio. However, two facts are clear from the results given. First, as fully expected, the range accrued during the coast period was found to be the predominant part of the total range. Thus, it may very well be possible to develop excellent suboptimal trajectories by using the same coasting phase with more practical thrusting phases (especially for the "dip" trajectories). Secondly, for larger amounts of fuel, the extremal trajectories deliver more units of range per unit mass of fuel; that is, for longer ranges, the trajectories are increasingly efficient.

Langley Research Center,
National Aeronautics and Space Administration,
Hampton, Va., May 27, 1970.

APPENDIX A

SOLUTION OF THE BOUNDARY-VALUE PROBLEM

The approach taken to obtain solutions of the boundary-value problem represented by equations (14) is an iterative method discussed in reference 5. In reference 5, for a similar boundary-value problem, a vector $\vec{e}(\vec{\alpha}, t_f)$ is defined so that when $\vec{e}(\vec{\alpha}, t_f) = \vec{0}$, the terminal boundary conditions are satisfied and the unknown initial conditions are $\vec{\alpha}$ where the arrows indicate vector quantities. For the problem at hand,

$$\vec{e}(\vec{\alpha}, t_f) = \begin{bmatrix} e_1(\vec{\alpha}, t_f) \\ e_2(\vec{\alpha}, t_f) \\ e_3(\vec{\alpha}, t_f) \end{bmatrix} = \begin{bmatrix} r(\vec{\alpha}, t_f) - r_0 \\ \dot{r}(\vec{\alpha}, t_f) \\ \dot{\theta}(\vec{\alpha}, t_f) \end{bmatrix} \quad (A1)$$

and

$$\vec{\alpha} = \begin{bmatrix} \alpha_1 \\ \alpha_2 \\ \alpha_3 \end{bmatrix} = \begin{bmatrix} p_1(t_0) \\ p_2(t_0) \\ p_4(t_0) \end{bmatrix} \quad (A2)$$

The argument $\vec{\alpha}$ is included in $r(\vec{\alpha}, t_f)$, $\dot{r}(\vec{\alpha}, t_f)$, and $\dot{\theta}(\vec{\alpha}, t_f)$ to indicate their implicit dependence on $\vec{\alpha}$ through equations (14) and also serves to indicate that a specific $\vec{\alpha}$ was used to obtain the value of the variable at t_f .

The magnitude of $\vec{e}(\vec{\alpha}, t_f)$ is measured by a scalar quantity

$$E[\vec{e}(\vec{\alpha}, t_f)] = \frac{\vec{e}(\vec{\alpha}, t_f)' B \vec{e}(\vec{\alpha}, t_f)}{2} \quad (A3)$$

where B is a positive definite diagonal matrix of weighting elements and primes denote a matrix transpose. Here

$$E[\vec{e}(\vec{\alpha}, t_f)] = \frac{1}{2} \left\{ b_1 [r(\vec{\alpha}, t_f) - r_0]^2 + b_2 \dot{r}^2(\vec{\alpha}, t_f) + b_3 \dot{\theta}^2(\vec{\alpha}, t_f) \right\} \quad (A4)$$

where

$$B = \text{diag}(b_1, b_2, b_3)$$

APPENDIX A – Continued

Initially, a value of $\bar{\alpha}$ is assumed, the differential equations (14) are integrated forward in time until the first time at which

$$m(t) - m_f = 0$$

and $\bar{e}(\bar{\alpha}, t_f)$ is evaluated. If $\bar{e}(\bar{\alpha}, t_f)$ vanishes, or, for numerical purposes, is sufficiently small, the boundary-value problem is considered to be solved. Otherwise, the assumed $\bar{\alpha}$ is corrected by

$$\delta\bar{\alpha} = - \left[\frac{\partial \bar{e}}{\partial \bar{\alpha}}(\bar{\alpha}, t_f)' B \frac{\partial \bar{e}}{\partial \bar{\alpha}}(\bar{\alpha}, t_f) + \gamma I_3 \right]^{-1} \frac{\partial \bar{e}}{\partial \bar{\alpha}}(\bar{\alpha}, t_f)' B \bar{e}(\bar{\alpha}, t_f) \quad (A5)$$

where the superscript -1 denotes a matrix inverse, I_3 is a 3 by 3 identity matrix, and $\gamma > 0$ is adjusted so that

$$E[\bar{e}(\bar{\alpha} + \delta\bar{\alpha}, t_f + \delta t_f)] < E[\bar{e}(\bar{\alpha}, t_f)] \quad (A6)$$

The increment δt_f is added to t_f in the expression (A6) since the final time for which $m(t) - m_f = 0$ by using $\bar{\alpha}$ may not be the same as that obtained by using $\bar{\alpha} + \delta\bar{\alpha}$. For this problem $\frac{\partial \bar{e}}{\partial \bar{\alpha}}(\bar{\alpha}, t_f)$ is a 3 by 3 matrix with elements a_{ij} ($i = 1, 2, 3; j = 1, 2, 3$) given by

$$\left. \begin{aligned} a_{1j} &= \frac{\partial r}{\partial \alpha_j}(\bar{\alpha}, t_f) \\ a_{2j} &= \frac{\partial \dot{r}}{\partial \alpha_j}(\bar{\alpha}, t_f) \\ a_{3j} &= \frac{\partial \dot{\theta}}{\partial \alpha_j}(\bar{\alpha}, t_f) \end{aligned} \right\} \quad (A7)$$

The quantities in equations (A7) are obtained by finding simultaneous solutions at t_f of equations (14) and a set of sensitivity equations derived as shown in reference 5 (p. 21, case (3c)) with t_f determined through

$$m(t) - m_f = 0$$

With the correction $\delta\bar{\alpha}$ computed, the assumed $\bar{\alpha}$ is replaced by $\bar{\alpha} + \delta\bar{\alpha}$ and the process is repeated by treating $\bar{\alpha} + \delta\bar{\alpha}$ as the assumed value.

APPENDIX A – Concluded

For the results of this paper, initial assumed values of $\bar{\alpha}$ were obtained by using a small amount of fuel and the results of reference 2 for the shorter trajectories and then using the $\bar{\alpha}$ from the last obtained solution as an initial guess for larger amounts of fuel. In each case

$$B = \text{diag}(1,1,1)$$

This approach for obtaining assumed values for $\bar{\alpha}$ is also suggested for values of initial thrust-weight ratio other than 5.0.

APPENDIX B

RELATIONSHIPS BETWEEN THE MAXIMUM RANGE AND MINIMUM FUEL PROBLEMS

In this section comparisons are drawn between the necessary conditions of the Pontryagin maximum principle as applied to the maximum-range—fixed-fuel and minimum-fuel—fixed-range problems. Each problem is for a rocket vehicle launched from rest and executing a soft landing on the surface of a spherical planet with an inverse-square-law gravity field.

The necessary conditions of both problems are summarized in the following chart. Conditions common to both problems are centered in the chart. The auxiliary variables of the maximum principle are denoted by p_i for the maximum-range—fixed-fuel problem and by λ_i for the minimum-fuel—fixed-range problem.

NECESSARY CONDITIONS FOR THE MAXIMUM RANGE AND MINIMUM FUEL PROBLEMS

Maximum Range-Fixed Fuel

Minimum Fuel-Fixed Range

The nondimensional dynamic equations for both problems are

$$\begin{array}{ll} \ddot{r} = \frac{T \cos \psi}{m} + r\dot{\theta}^2 - \mu/r^2 & \left(r(t_0) = r(t_f) = r_0, \dot{r}(t_0) = \dot{r}(t_f) = 0 \right) \\ \ddot{\theta} = \frac{T \sin \psi}{rm} - \frac{2\dot{r}\dot{\theta}}{r} & \left(\theta(t_0) = \theta(t_f) = \theta_0 \right) \\ \dot{m} = -T & \left(m(t_0) = m_0 \right) \end{array}$$

where $0 \leq T \leq 1$, t_f unspecified

$(\theta(t_f) \text{ maximized, } m(t_f) \text{ specified})$

$(\theta(t_f) \text{ specified, } m_0 - m_f \text{ minimized})$

In integral form minimize

$$\begin{array}{ll} \int_{t_0}^{t_f} \dot{\theta} dt & \int_{t_0}^{t_f} \dot{m} dt \end{array}$$

Application of the Pontryagin Maximum Principle leads to the
necessary conditions

$$T = \begin{cases} 1 & (f_s > 0) \\ 0 & (f_s < 0) \end{cases}$$

APPENDIX B - Continued

where

$$f_s = \frac{p_2 \cos \psi}{m} + \frac{p_4 \sin \psi}{rm} - p_5$$

$$f_s = \frac{\lambda_2 \cos \psi}{m} + \frac{\lambda_4 \sin \psi}{rm} - (\lambda_5 - \lambda_0)$$

and for $T \neq 0$

$$\cos \psi = \frac{p_2}{\sqrt{p_2^2 + (p_4/r)^2}}$$

$$\cos \psi = \frac{\lambda_2}{\sqrt{\lambda_2^2 + (\lambda_4/r)^2}}$$

$$\sin \psi = \frac{p_4}{r \sqrt{p_2^2 + (p_4/r)^2}}$$

$$\sin \psi = \frac{\lambda_4}{r \sqrt{\lambda_2^2 + (\lambda_4/r)^2}}$$

with

$$p_0 \leq 0$$

$$\lambda_0 \leq 0$$

$$\dot{p}_1 = -p_2 \dot{\theta}^2 - 2p_2 \frac{\mu}{r^3} - 2p_4 \frac{\dot{r}\dot{\theta}}{r^2} + T \frac{p_4 \sin \psi}{mr^2}$$

$$\dot{\lambda}_1 = -\lambda_2 \dot{\theta}^2 - \frac{2\lambda_2 \mu}{r^3} - \frac{2\lambda_4 \dot{r}\dot{\theta}}{r^2} + \frac{T\lambda_4 \sin \psi}{mr^2}$$

$$\dot{p}_2 = -p_1 + \frac{2p_4 \dot{\theta}}{r}$$

$$\dot{\lambda}_2 = -\lambda_1 + 2\lambda_4 \frac{\dot{\theta}}{r}$$

$$\dot{p}_3 = 0 \quad \left(p_3(t_f) = 0 \right)$$

$$\dot{\lambda}_3 = 0$$

$$\dot{p}_4 = -(p_3 - p_0) - 2p_2 r \dot{\theta} + 2p_4 \frac{\dot{r}}{r}$$

$$\dot{\lambda}_4 = -\lambda_3 - 2\lambda_2 r \dot{\theta} + 2\lambda_4 \frac{\dot{r}}{r}$$

$$\dot{p}_5 = \frac{T}{m^2} \left(p_2 \cos \psi + \frac{p_4 \sin \psi}{r} \right)$$

$$\dot{\lambda}_5 = \frac{T}{m^2} \left(\lambda_2 \cos \psi + \frac{\lambda_4 \sin \psi}{r} \right) \quad \left(\lambda_5(t_f) = 0 \right)$$

$$H = p_1 \dot{r} + p_2 \left(r \dot{\theta}^2 + \frac{T \cos \psi}{m} - \frac{\mu}{r^2} \right)$$

$$H = \lambda_1 \dot{r} + \lambda_2 \left(r \dot{\theta}^2 + \frac{T \cos \psi}{m} - \frac{\mu}{r^2} \right)$$

$$+ (p_3 - p_0) \dot{\theta} + p_4 \left(\frac{T \sin \psi}{rm} - \frac{2r\dot{\theta}}{r} \right)$$

$$+ \lambda_3 \dot{\theta} + \lambda_4 \left(\frac{T \sin \psi}{rm} - \frac{2r\dot{\theta}}{r} \right)$$

$$- p_5 T \equiv 0$$

$$- (\lambda_5 - \lambda_0) T \equiv 0$$

Given an extremal maximum range solution with specified fuel expenditure $m_0 - m_f$ and $p_5(t_f) \geq 0$, this same solution can be made to satisfy the necessary conditions for fuel optimality between the maximum range launch and landing points with extremal fuel given by $m_0 - m_f$ by making the identification

$$\lambda_i(t) = p_i(t) \quad (i = 1, 2, 4)$$

$$\lambda_3(t) = p_3(t) - p_0$$

$$\lambda_5(t) - \lambda_0 = p_5(t)$$

APPENDIX B – Concluded

In order to satisfy $\lambda_5(t_f) = 0$, let

$$\lambda_0 = -p_5(t_f)$$

Also $\lambda_3(t_f) = -p_0$ follows from $p_3(t_f) = 0$.

Likewise, if given an extremal minimum fuel solution with extremal final mass m_f , specified range angle $\theta(t_f)$, and $\lambda_3(t_f) \geq 0$, this same solution can be made to satisfy the necessary conditions for maximal range with specified final mass m_f and extremal range angle $\theta(t_f)$ by making the identification

$$p_i(t) = \lambda_i(t) \quad (i = 1, 2, 4)$$

$$p_3(t) - p_0 = \lambda_3(t)$$

$$p_5(t) = \lambda_5(t) - \lambda_0$$

In order to satisfy $p_3(t_f) = 0$, let

$$p_0 = -\lambda_3(t_f)$$

Each of the maximum range extremals presented as results in this paper had $p_5(t_f) > 0$ whereby they are minimum fuel extremals.

The program may thus be used to construct minimum fuel extremals by finding a maximum range extremal which achieves the desired range and then checking to determine whether $p_5(t_f) > 0$.

REFERENCES

1. Manci, Orlando J., Jr.: Minimum Fuel Trajectories With Soft Landings. SRL 64-3, U.S. Air Force, May 30, 1964. (Available from DDC as AD 447904.)
2. Childs, A. Gary; and Armstrong, Ernest S.: Analysis of Maximum Range Trajectories for Rocket-Propelled Lunar Flying Vehicles in a Uniform Gravitational Field. NASA TN D-5475, 1969.
3. Needham, Kenneth E.: Minimum Fuel Trajectories for Thrust Limited Rockets in an Inverse Square Gravity Field. GA/Mech/65-38, Air Force Inst. Technol., Aug. 1965. (Available from DDC as AD 625 395.)
4. Pontryagin, L. S.; Boltyanskii, V. G.; Gamkrelidze, R. V.; and Mishchenko, E. F.: The Mathematical Theory of Optimal Processes. Interscience Publ., Inc., c.1962.
5. Armstrong, Ernest S.: A Combined Newton-Raphson and Gradient Parameter Correction Technique for Solution of Optimal Control Problems. NASA TR R-293, 1968.
6. Armstrong, Ernest S.; and Markos, Athena T.: A Computational Method for Time-Optimal Space Rendezvous. NASA TN D-5017, 1969.
7. Straeter, Terrance A.: A Comparison of Gradient Dependent Techniques for the Minimization of an Unconstrained Function of Several Variables. Paper presented at AIAA Aerospace Computer Systems Conference (Los Angeles, Calif.), Sept. 1969.
8. Kopp, Richard E.: Pontryagin Maximum Principle. Optimization Techniques With Applications to Aerospace Systems, George Leitmann, ed., Academic Press, Inc., c.1962, pp. 255-279.
9. Kelley, Henry J.; Kopp, Richard E.; and Moyer, H. Gardner: Singular Extremals. Topics in Optimization, George Leitmann, ed., Academic Press, Inc., c.1967, pp. 63-101.
10. Hsu, Jay C.; and Meyer, Andrew U.: Modern Control Principles and Applications. McGraw-Hill Book Co., Inc., c.1968.

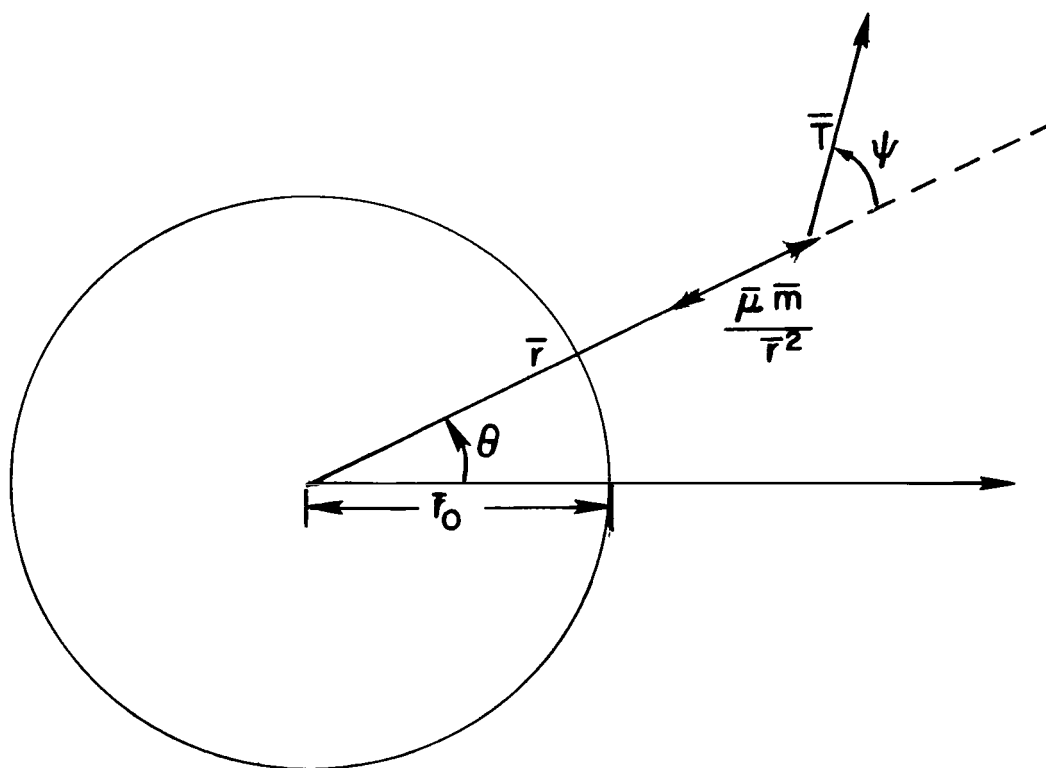


Figure 1.- Coordinate system for inverse-square-law gravity-field maximum-range problem.
Polar coordinates, \bar{r}, θ ; thrust components \bar{T}, ψ ; and gravity force $\mu \bar{m} / \bar{r}^2$.

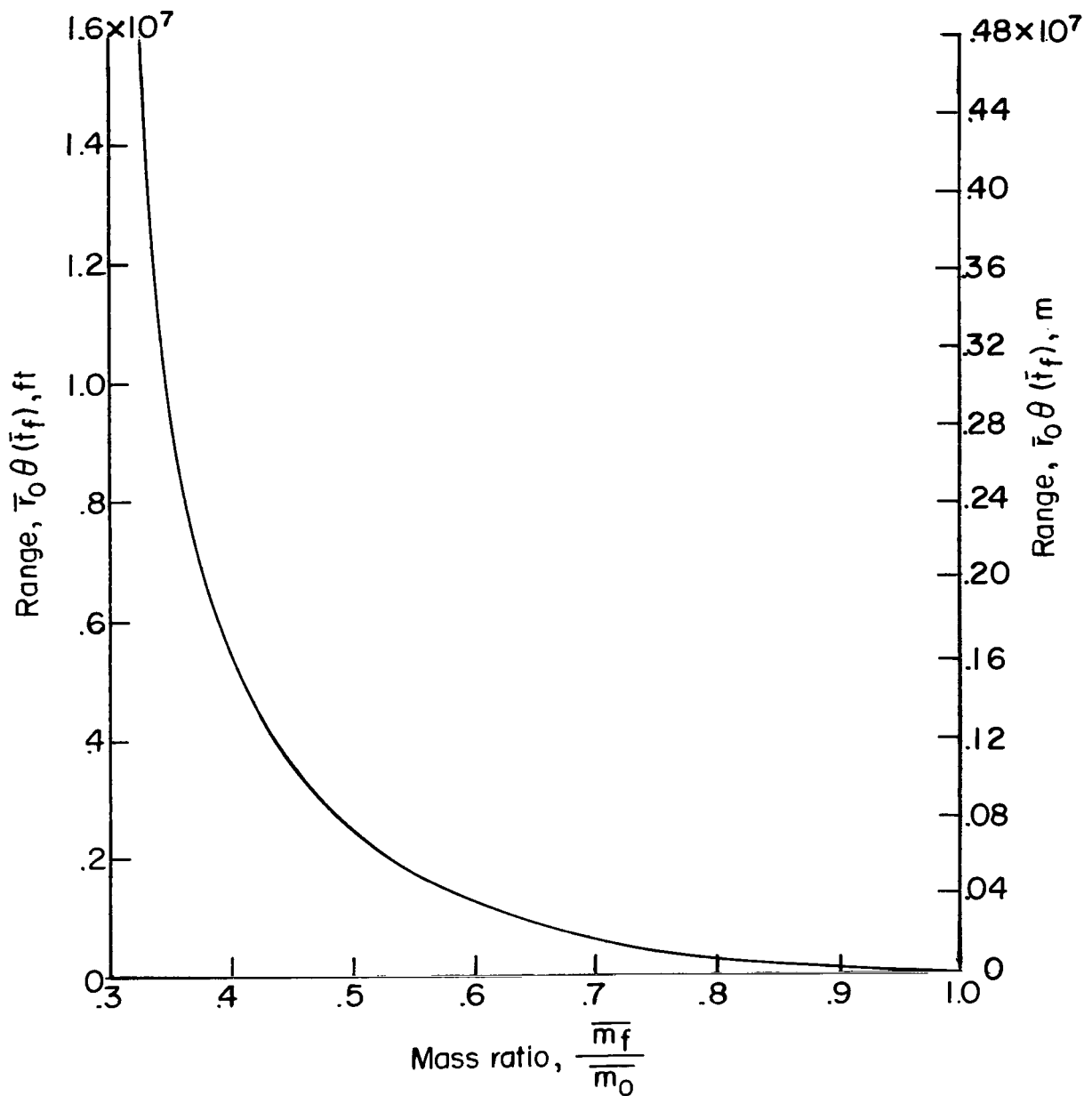


Figure 2.- Range as a function of the ratio of final mass to initial mass \bar{m}_f/\bar{m}_0 .

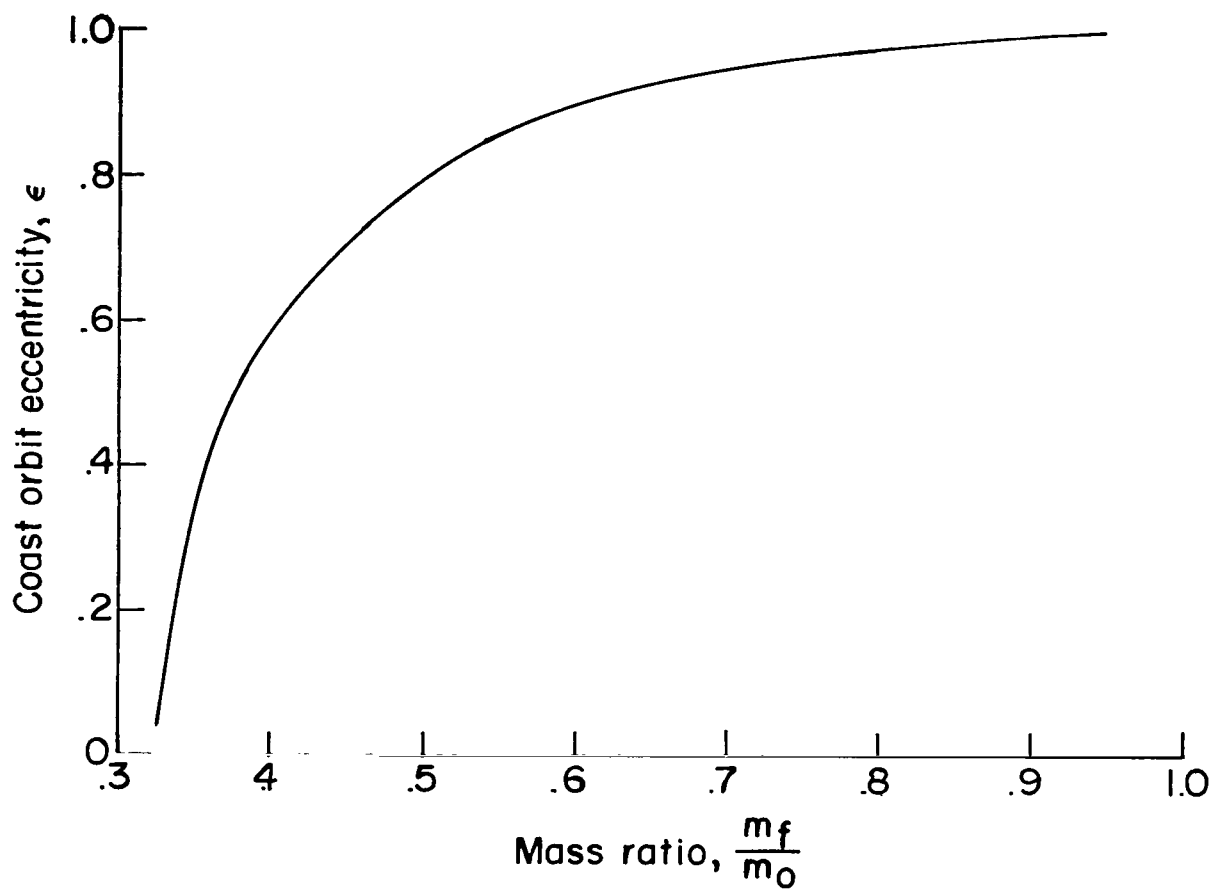


Figure 3.- Coast orbit eccentricity as a function of the ratio of final mass to initial mass.

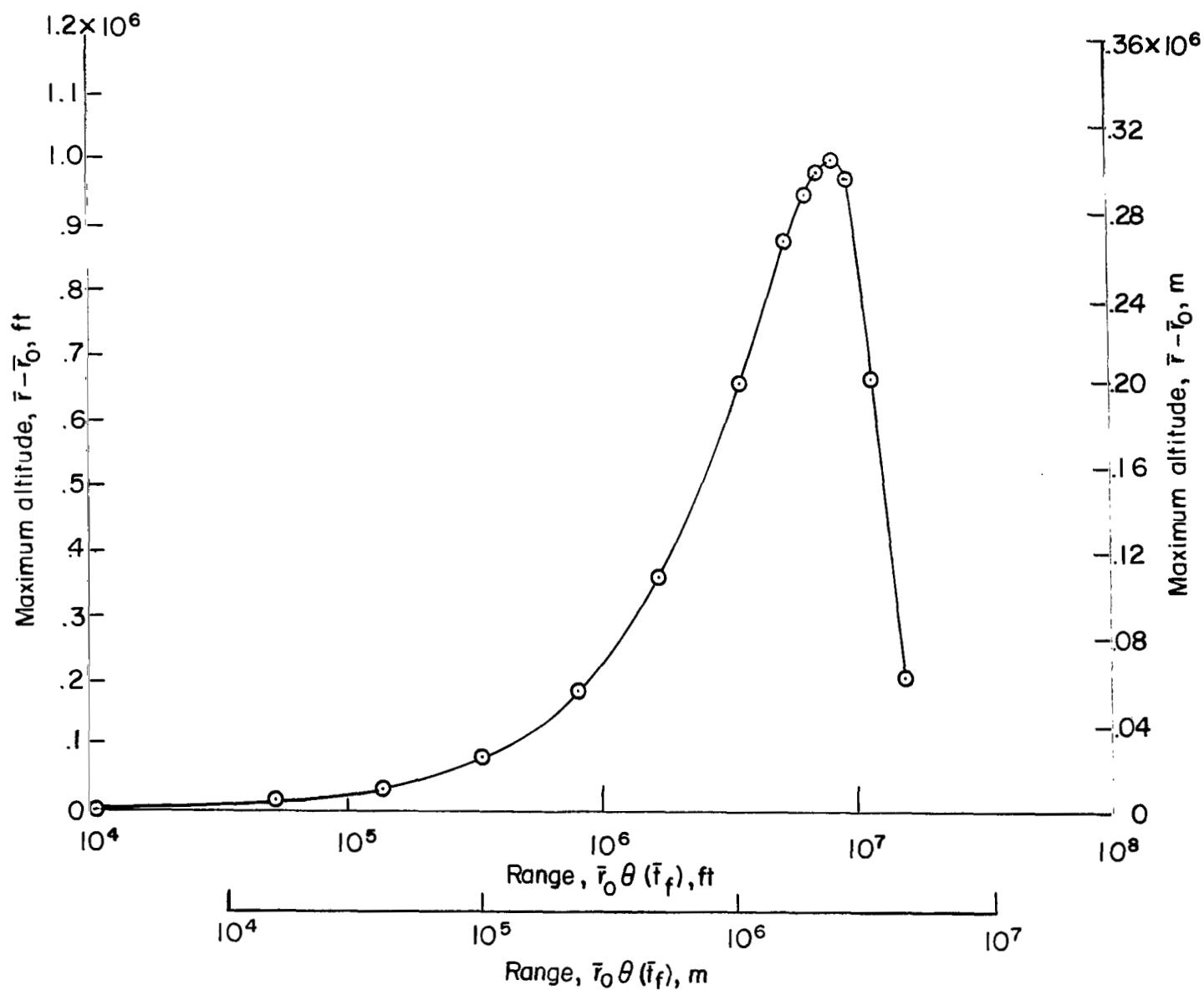


Figure 4.- Altitude as a function of range.

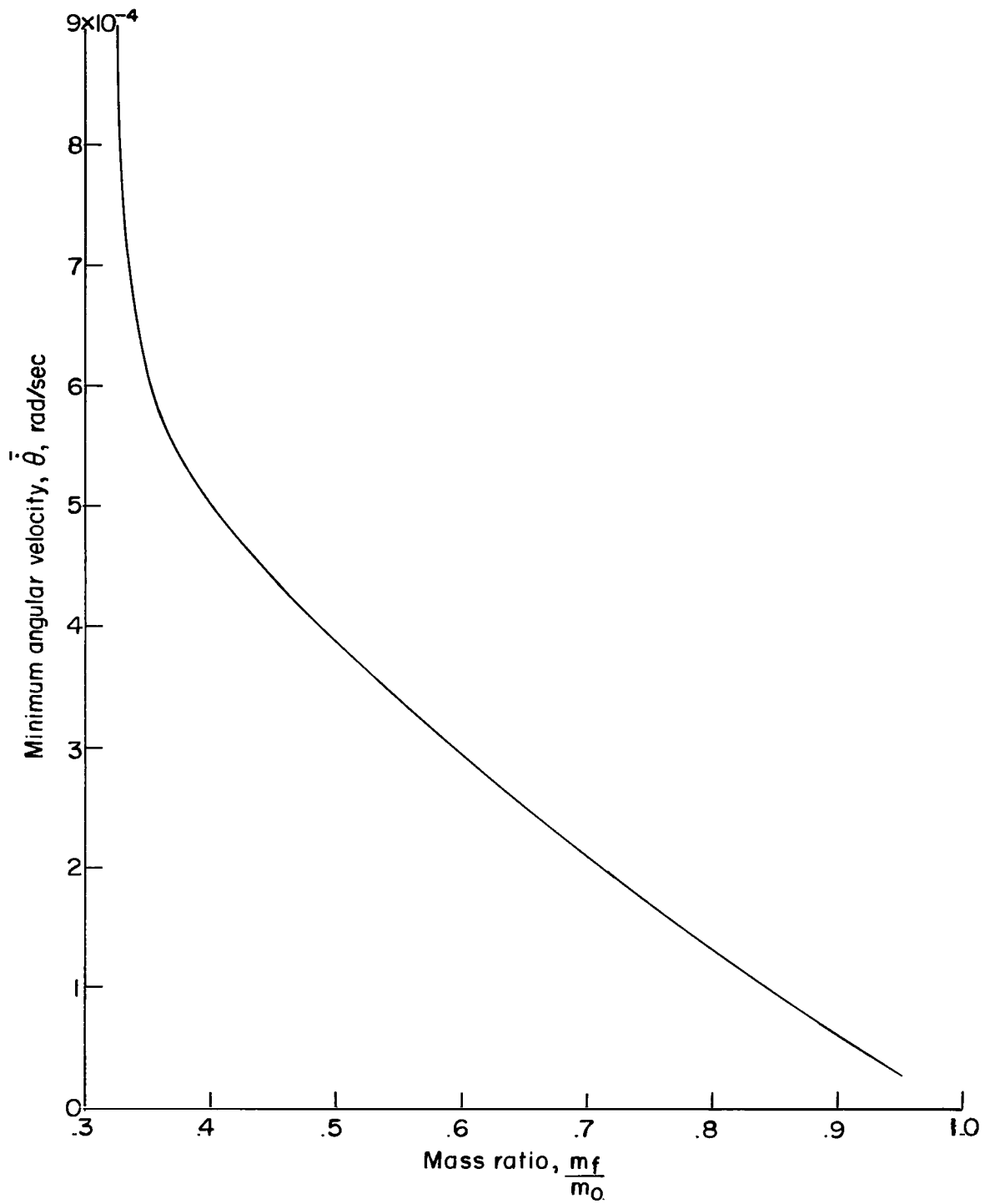
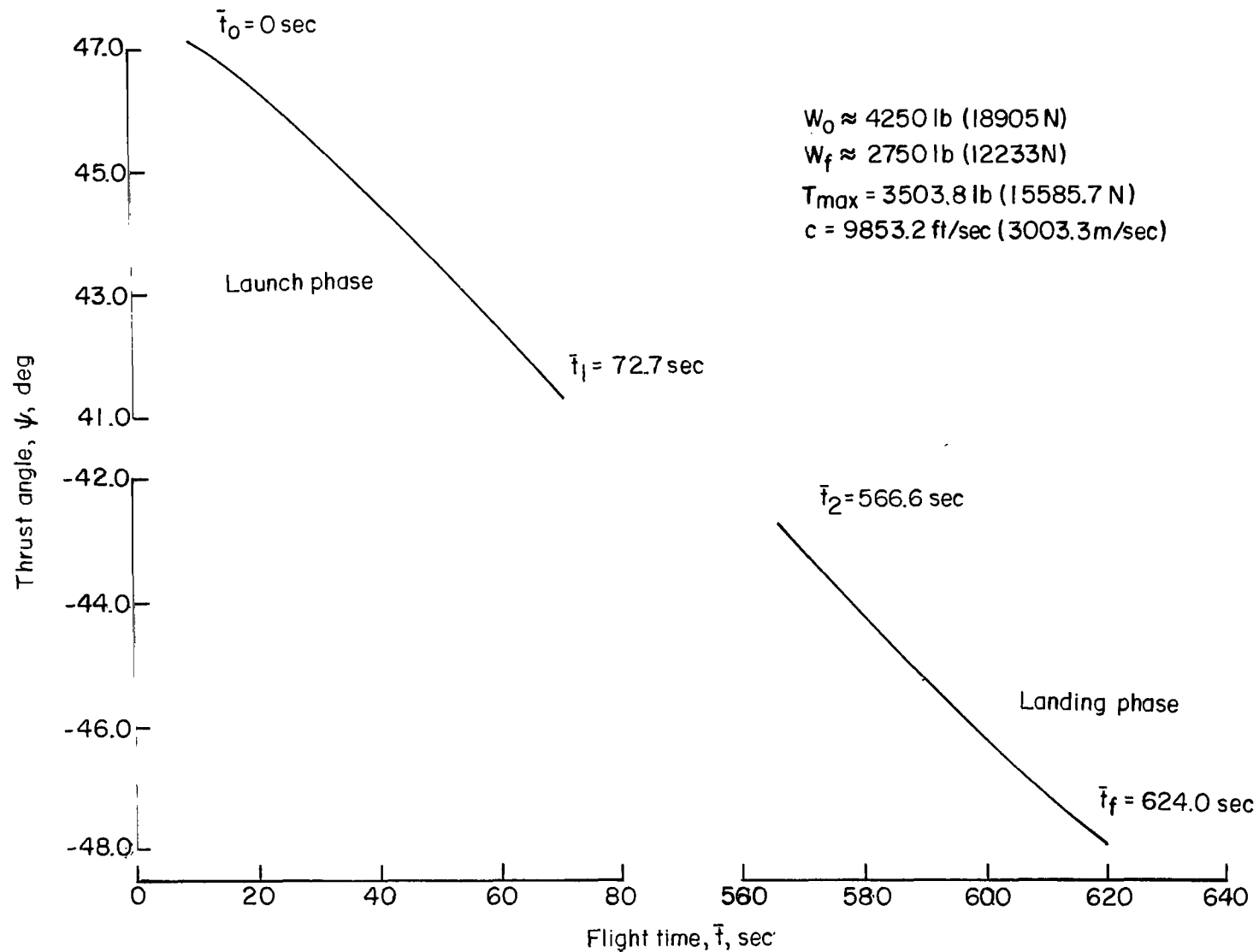
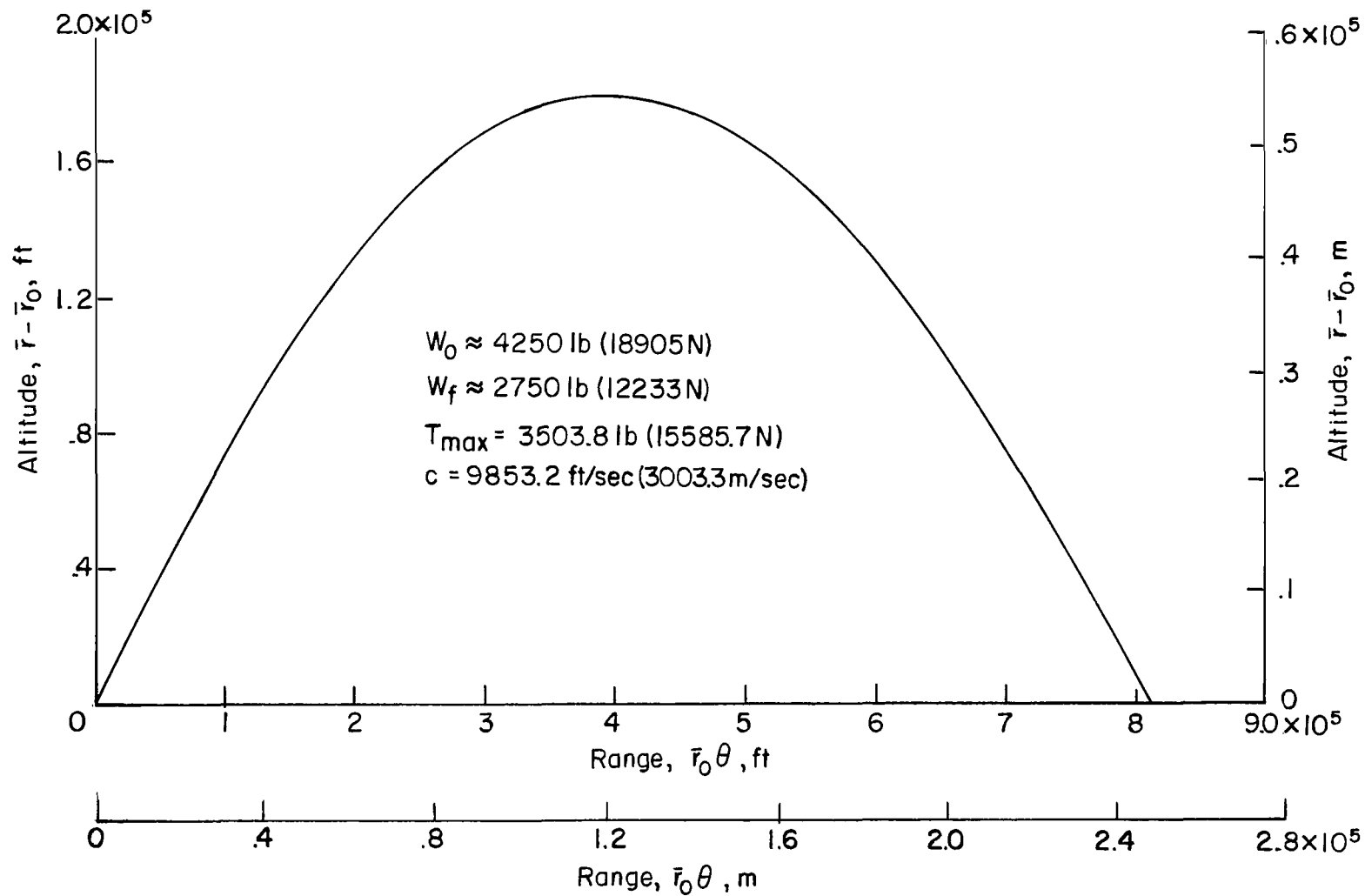


Figure 5.- Minimum angular velocity during the coast phase as a function of the ratio of final mass to initial mass.



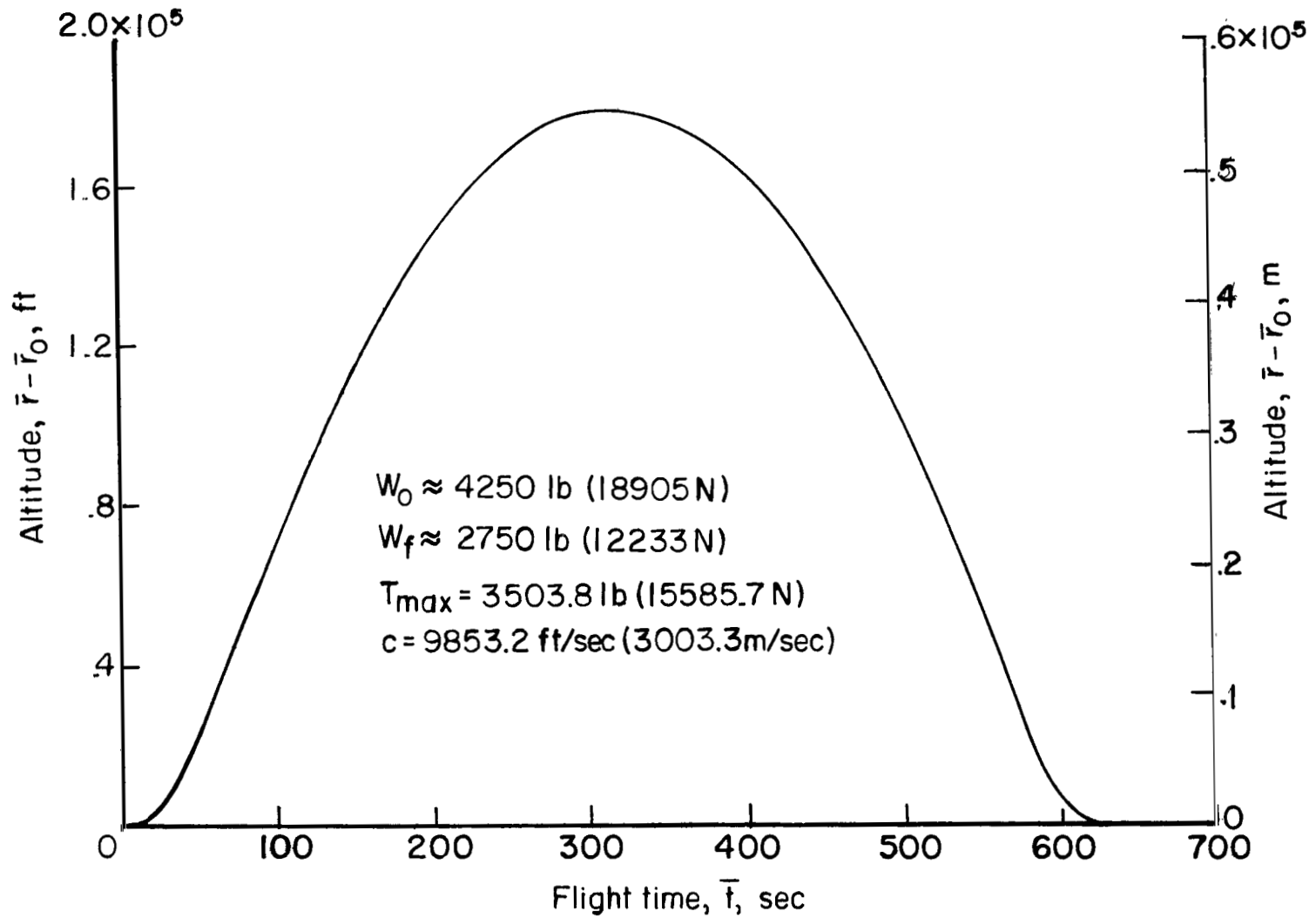
(a) Variation of thrust angle with time. (ψ is measured from the vertical direction as shown in fig. 1.)

Figure 6.- Optimal control and trajectories. $m_f/m_0 = 0.65$.



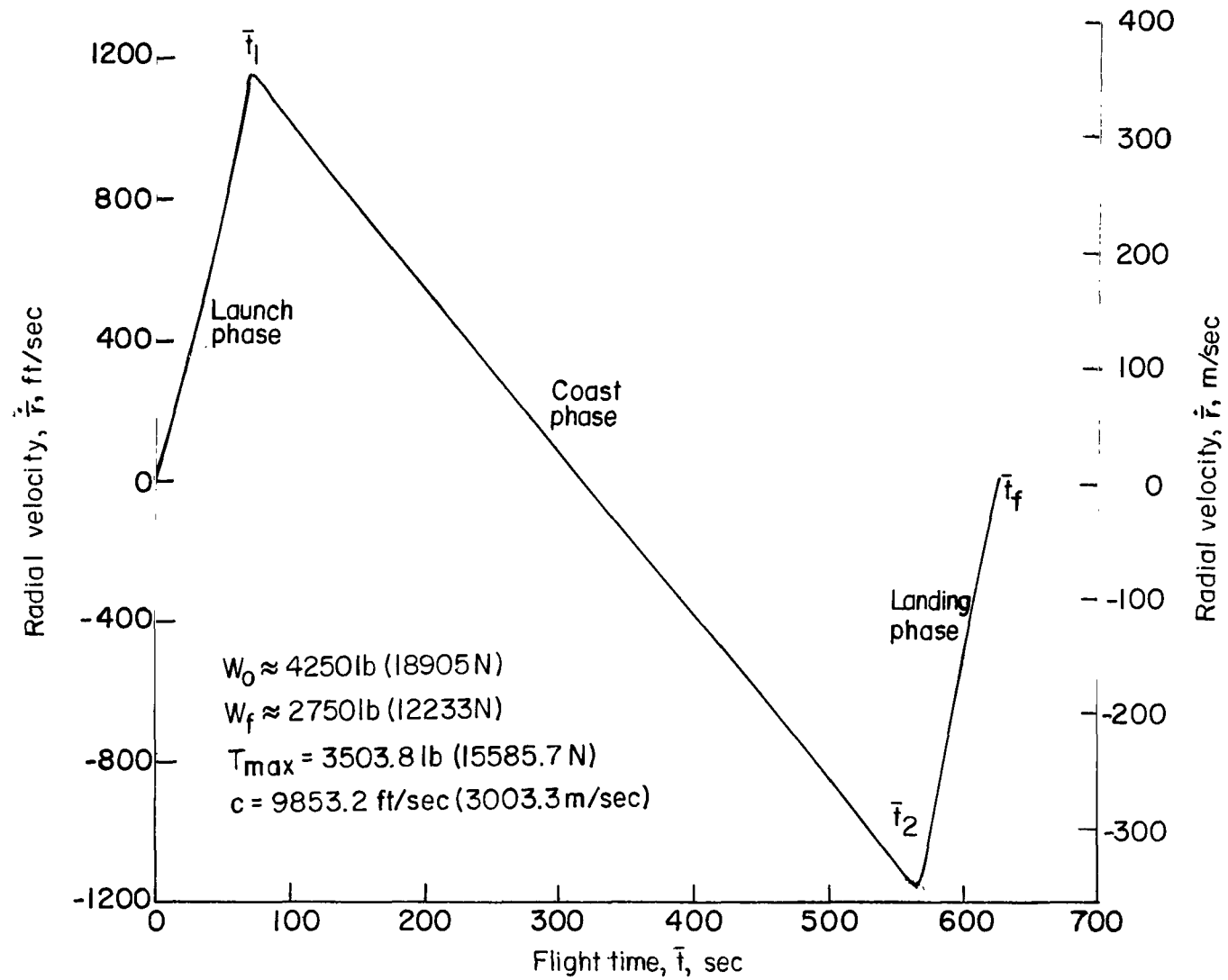
(b) Variation of altitude with range.

Figure 6.- Continued.



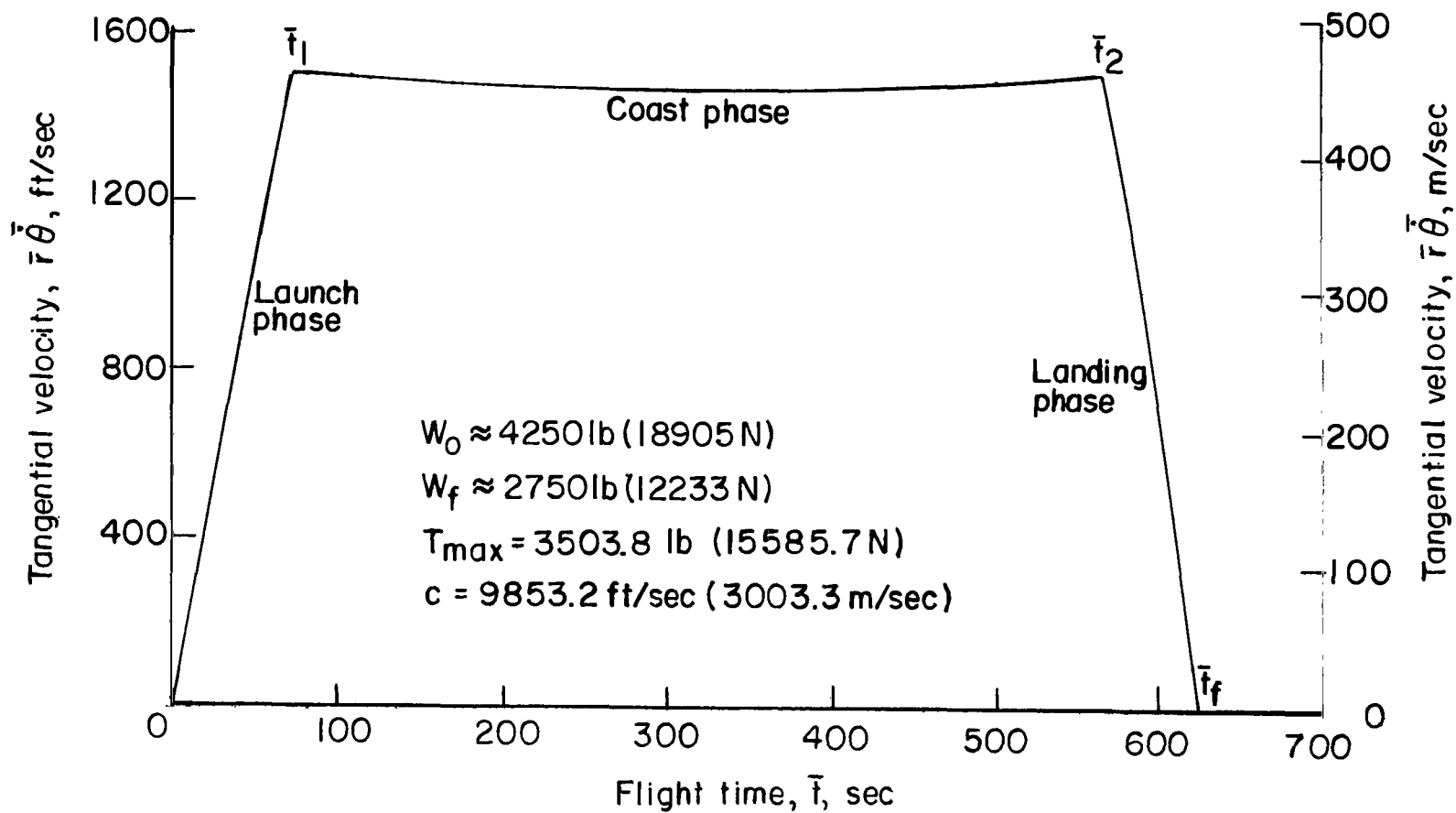
(c) Variation of altitude with time.

Figure 6.- Continued.



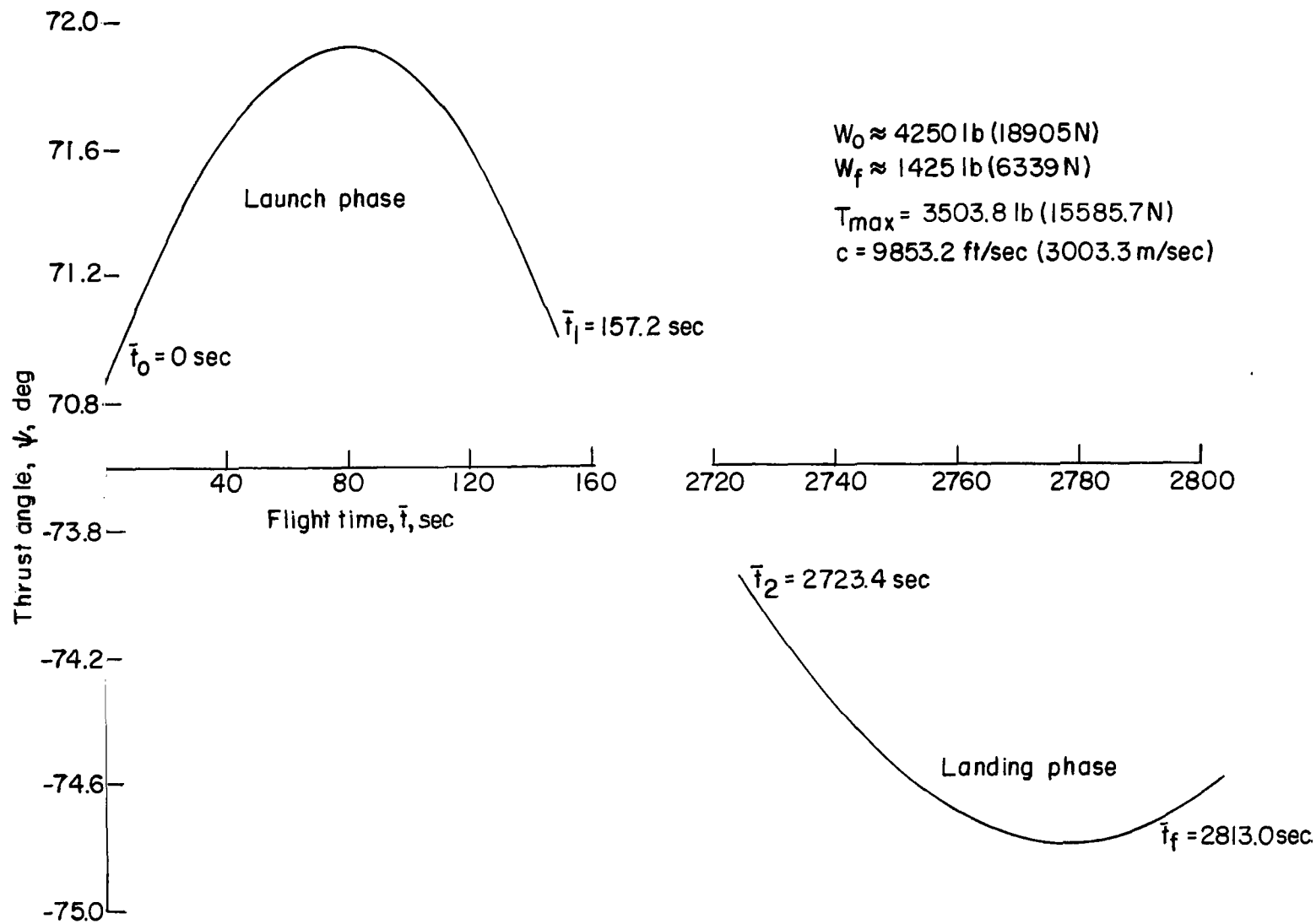
(d) Variation of radial velocity with time.

Figure 6.- Continued.



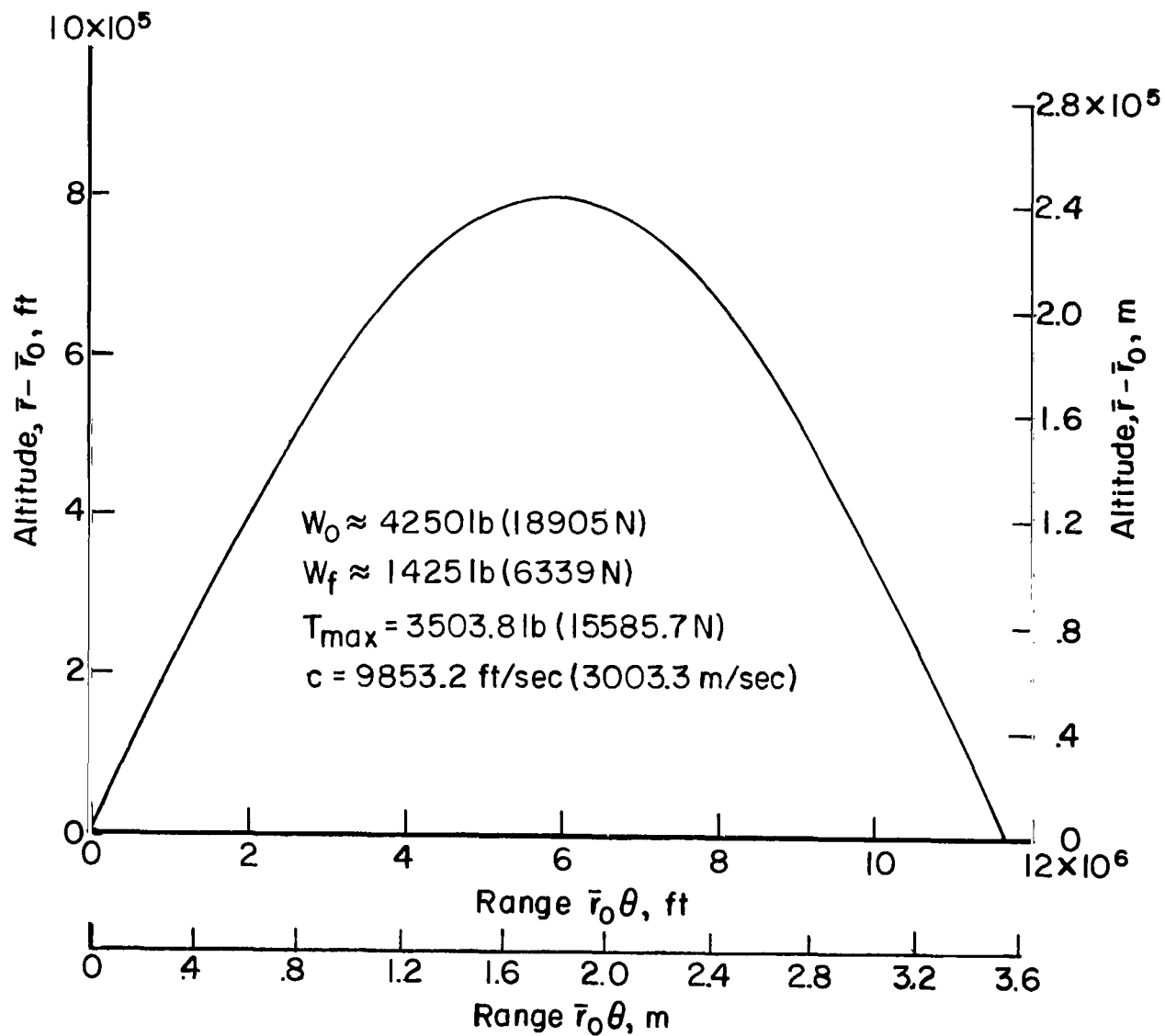
(e) Variation of tangential velocity with time.

Figure 6.- Concluded.



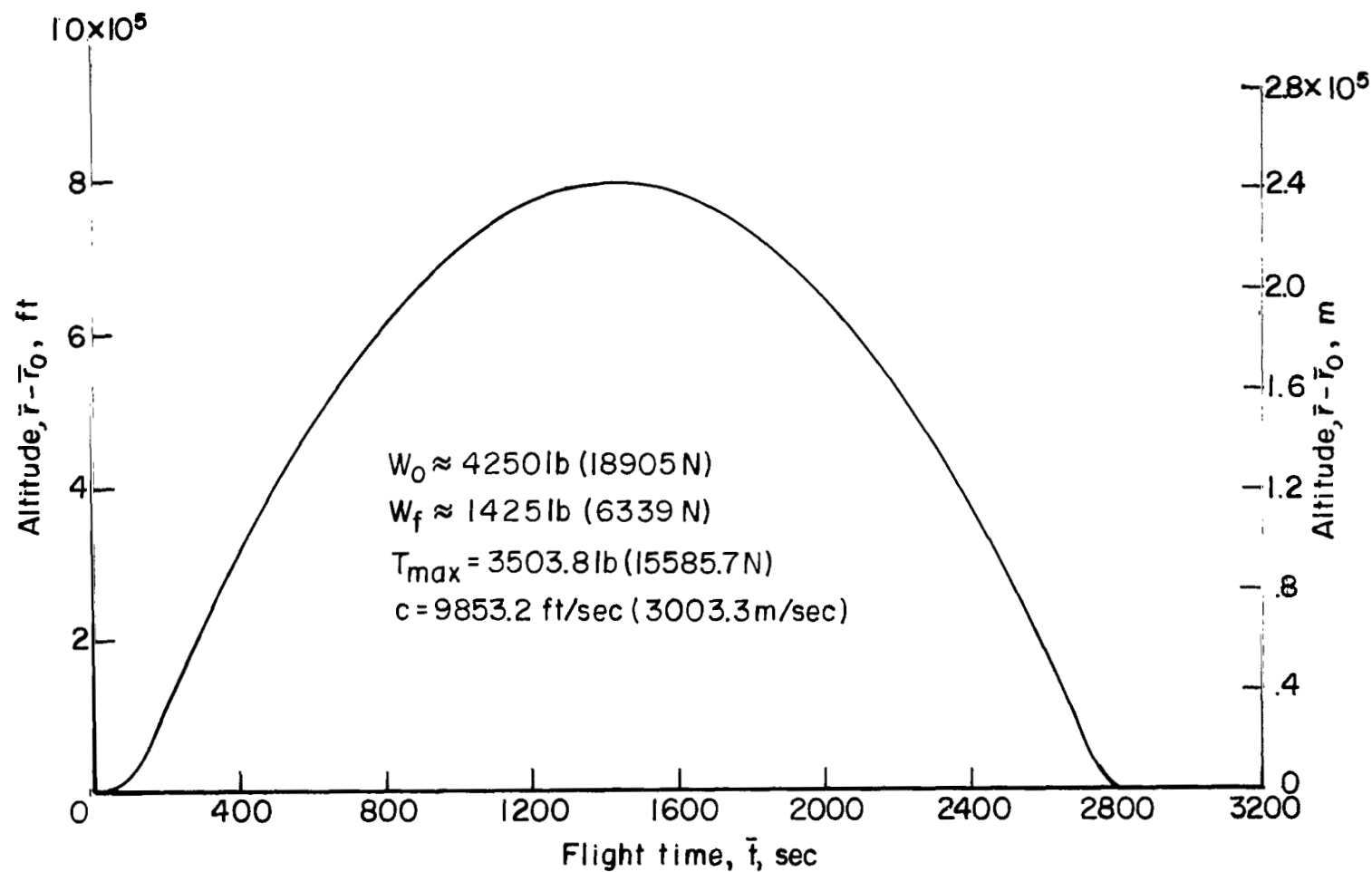
(a) Variation of thrust angle with time. (ψ is measured from the vertical direction as shown in fig. 1.)

Figure 7.- Optimal control and trajectories, $m_f/m_0 = 0.335$.



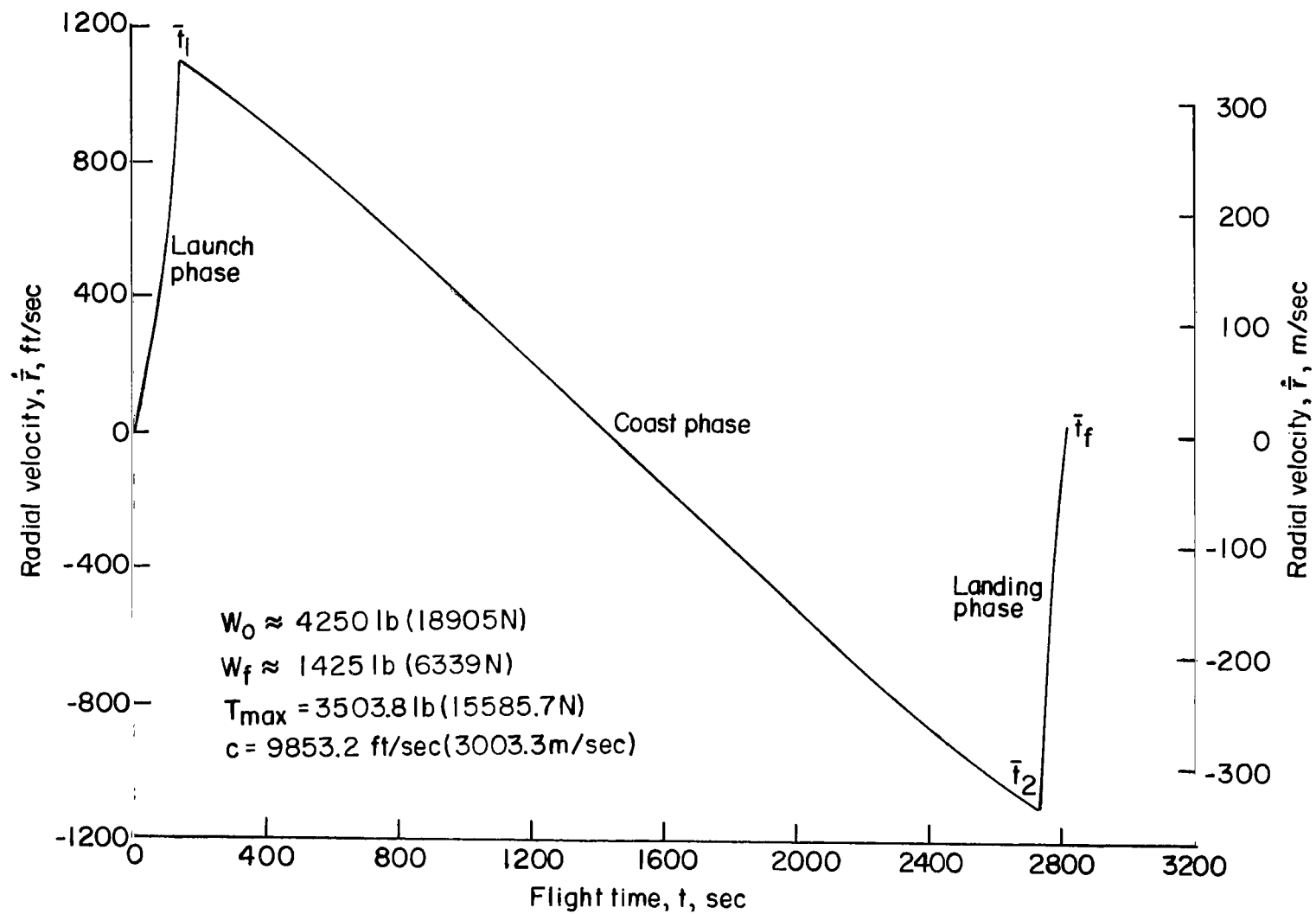
(b) Variation of altitude with range.

Figure 7.- Continued.



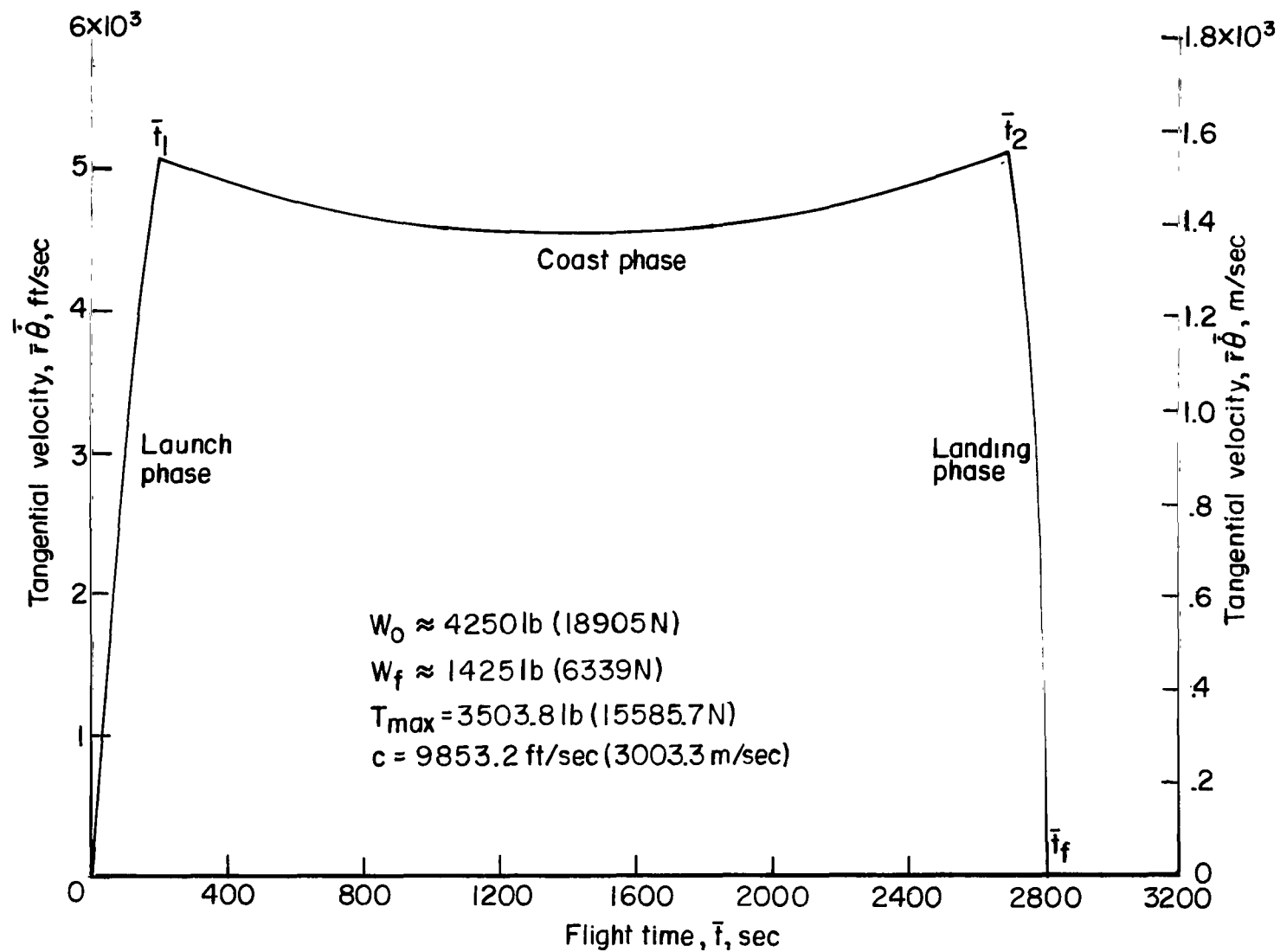
(c) Variation of altitude with time.

Figure 7.- Continued.



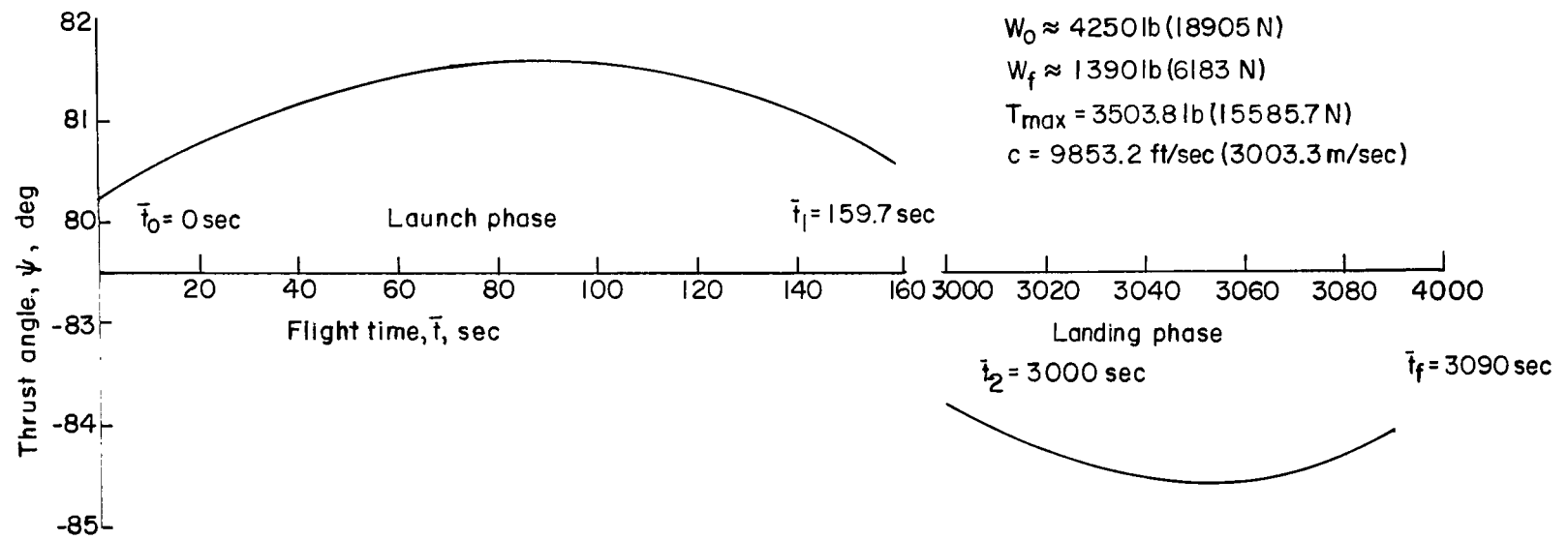
(d) Variation of radial velocity with time.

Figure 7.- Continued.



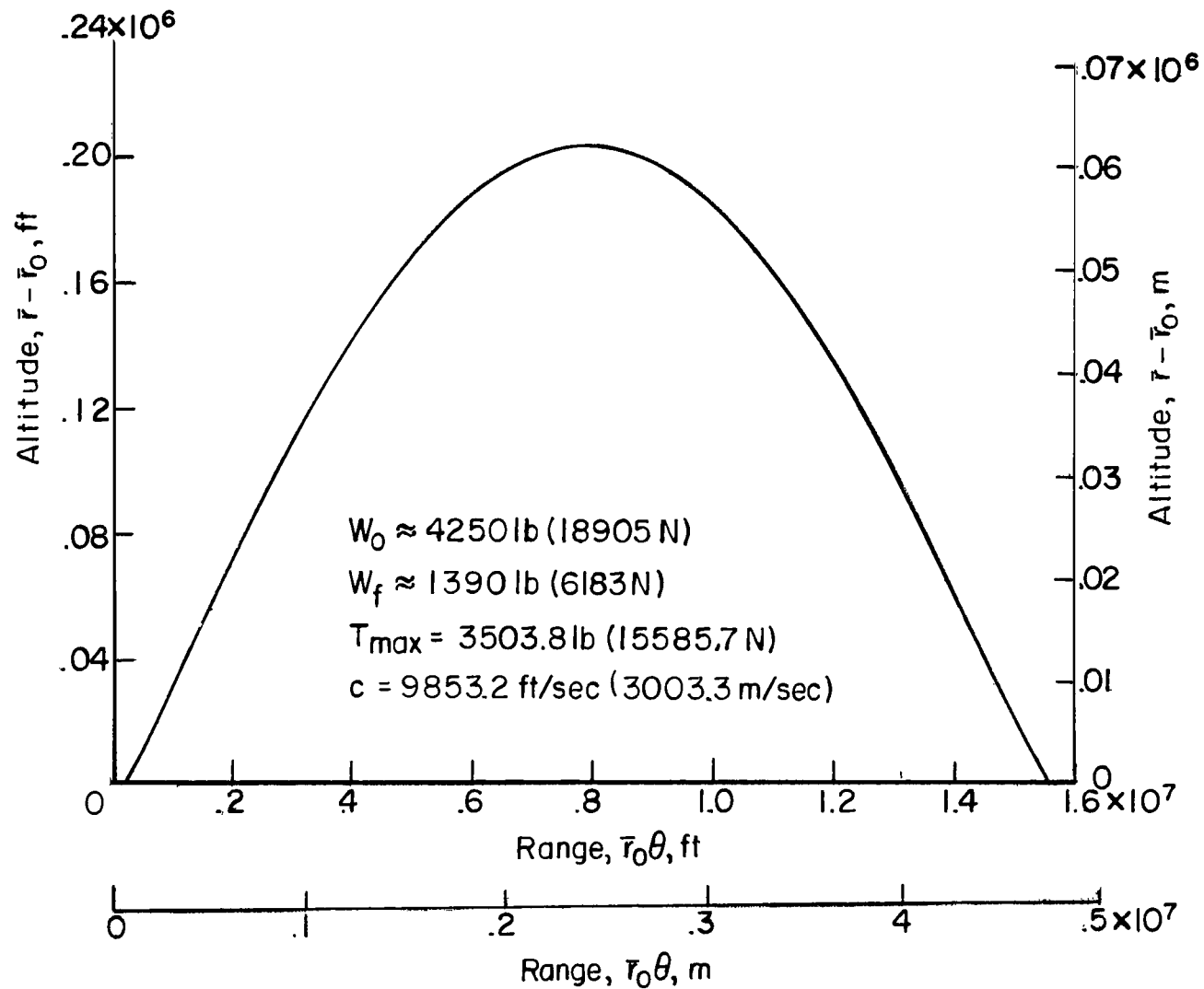
(e) Variation of tangential velocity with time.

Figure 7.- Concluded.



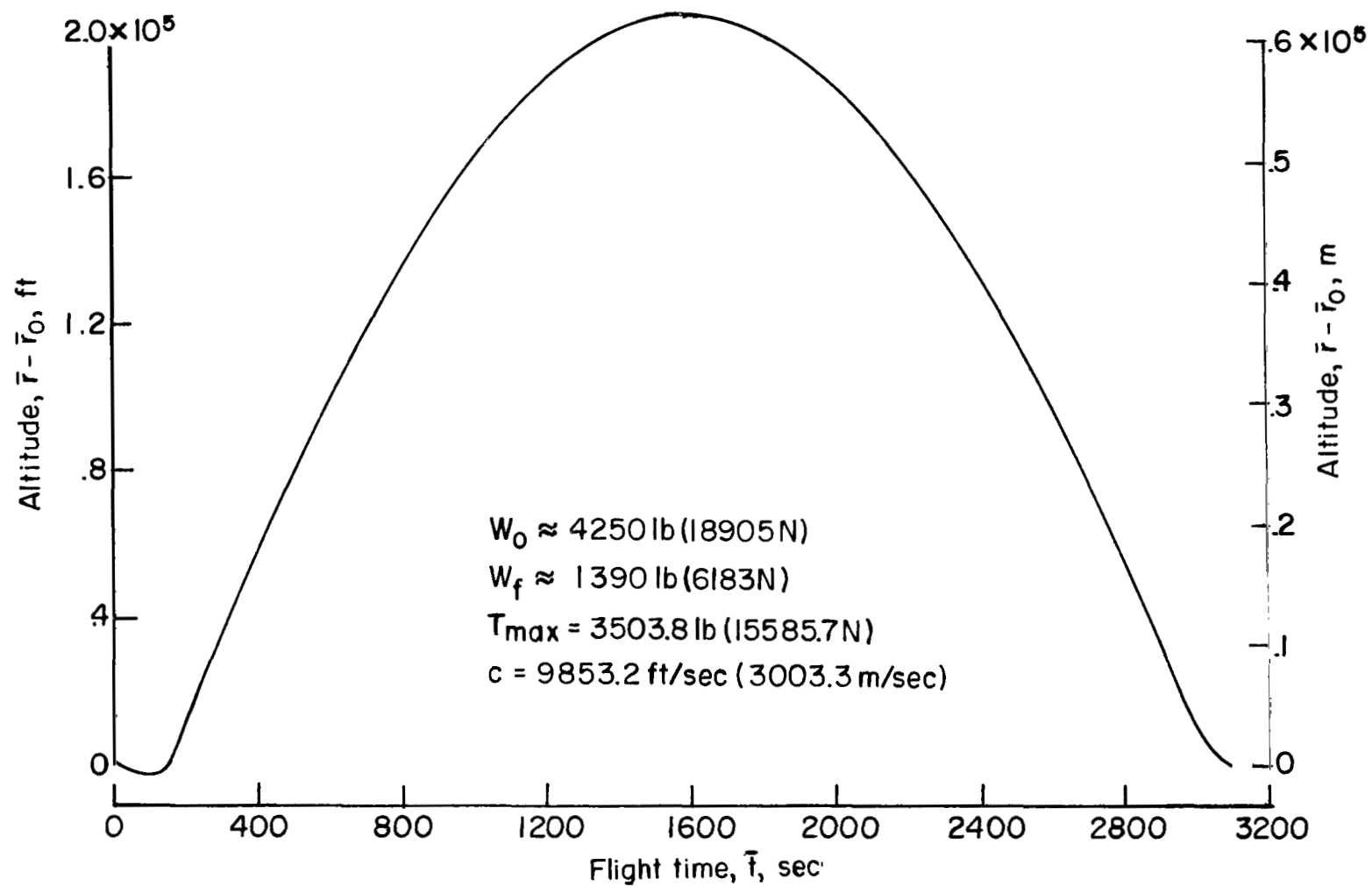
(a) Variation of thrust angle with time. (ψ is measured from the vertical direction as shown in fig. 1.)

Figure 8.- Optimal control and trajectories. $m_f/m_0 = 0.326$.



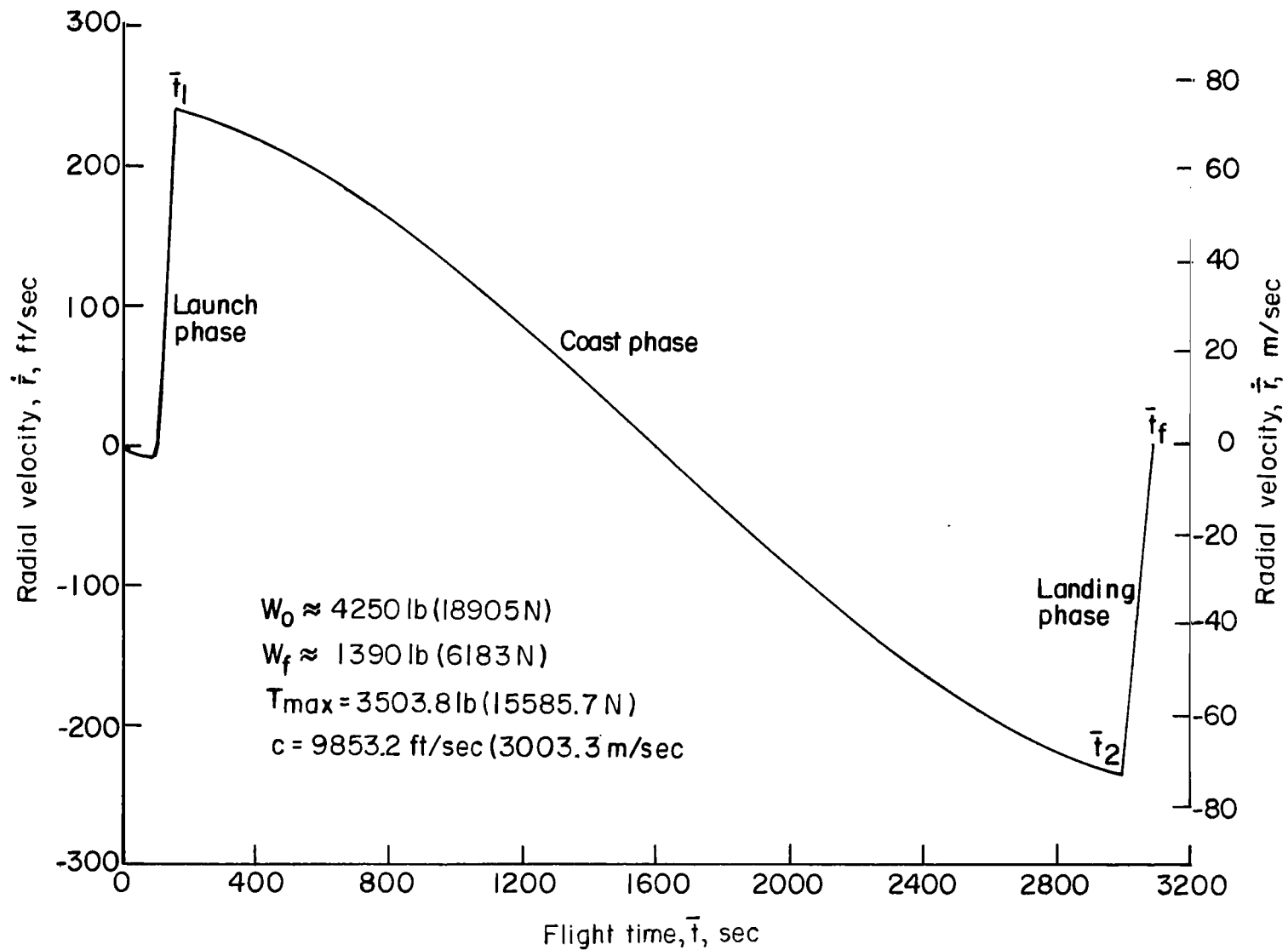
(b) Variation of altitude with range.

Figure 8.- Continued.



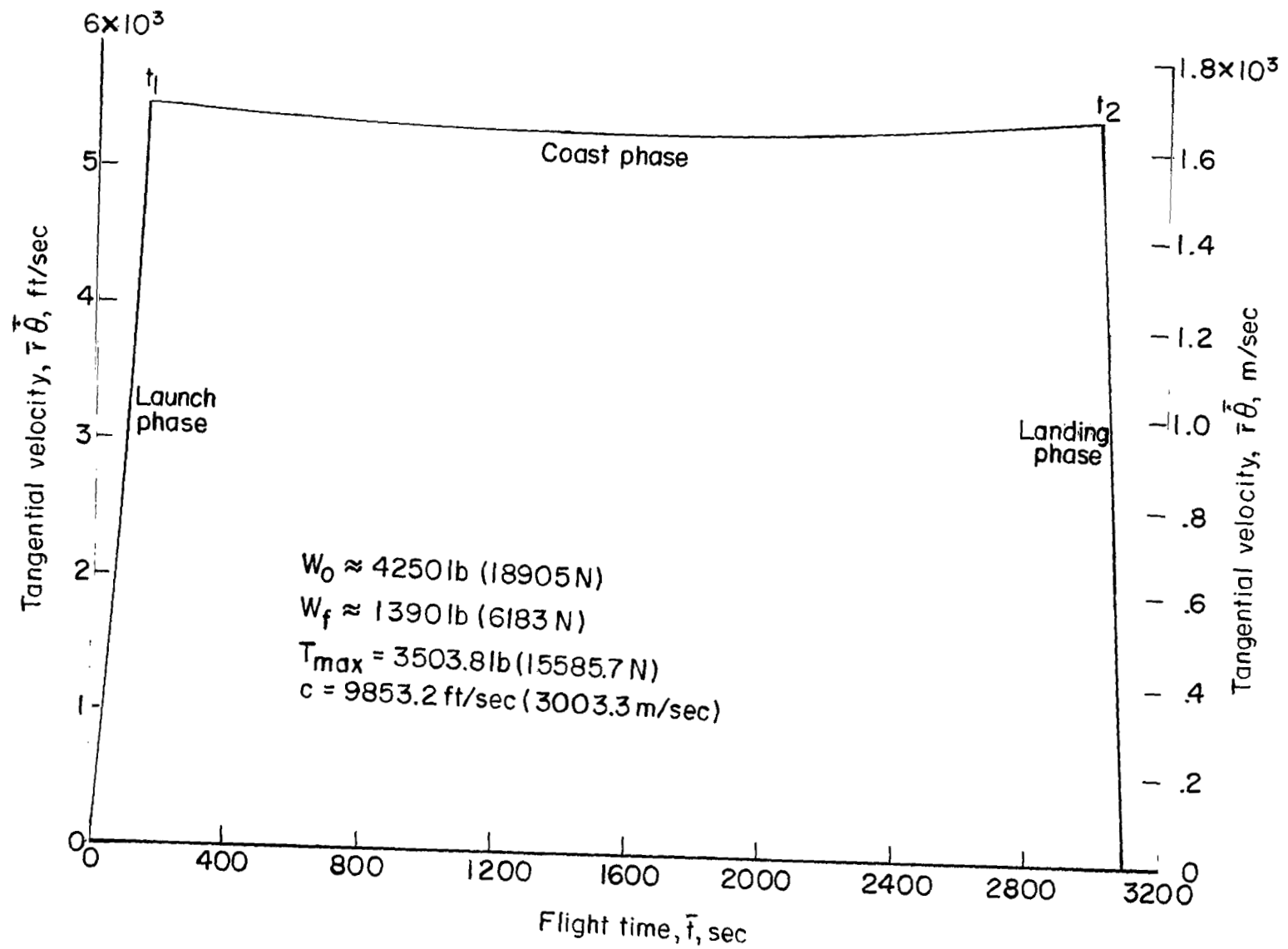
(c) Variation of altitude with time.

Figure 8.- Continued.



(d) Variation of radial velocity with time.

Figure 8.- Continued.



(e) Variation of tangential velocity with time.

Figure 8.- Concluded.

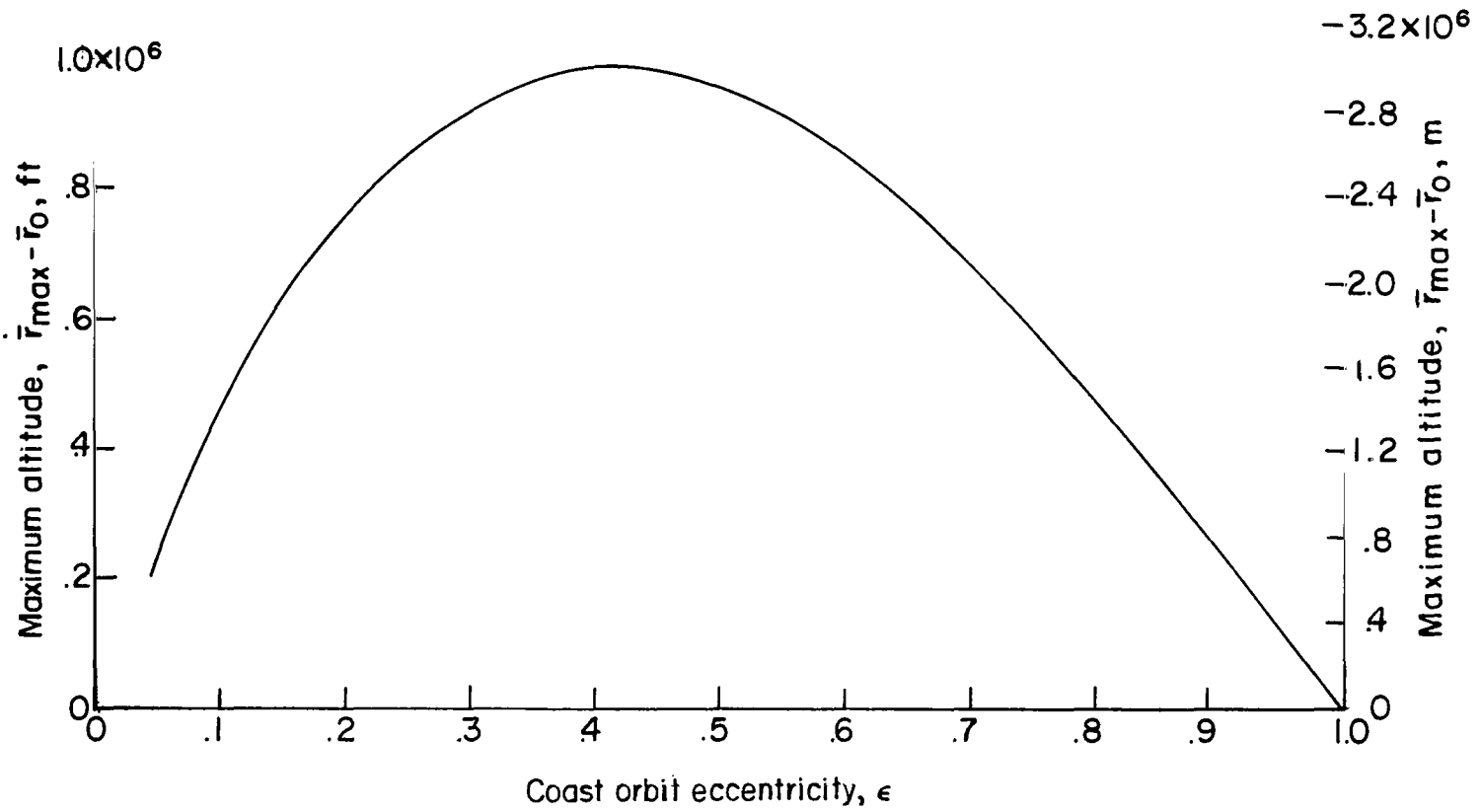


Figure 9.- Maximum altitude $r_{\max} - r_0$ as a function of the coast orbit eccentricity ϵ .

NATIONAL AERONAUTICS AND SPACE ADMINISTRATION

WASHINGTON, D. C. 20546

OFFICIAL BUSINESS

FIRST CLASS MAIL



POSTAGE AND FEES PAID
NATIONAL AERONAUTICS AND
SPACE ADMINISTRATION

03U 001 55 51 3DS 00903
AIR FORCE WEAPONS LABORATORY /WLOL/
KIRTLAND AFB, NEW MEXICO 87117

ATT E. LOU BOWMAN, CHIEF, TECH. LIBRARY

POSTMASTER: If Undeliverable (Section 158
Postal Manual) Do Not Return

"The aeronautical and space activities of the United States shall be conducted so as to contribute . . . to the expansion of human knowledge of phenomena in the atmosphere and space. The Administration shall provide for the widest practicable and appropriate dissemination of information concerning its activities and the results thereof."

— NATIONAL AERONAUTICS AND SPACE ACT OF 1958

NASA SCIENTIFIC AND TECHNICAL PUBLICATIONS

TECHNICAL REPORTS: Scientific and technical information considered important, complete, and a lasting contribution to existing knowledge.

TECHNICAL NOTES: Information less broad in scope but nevertheless of importance as a contribution to existing knowledge.

TECHNICAL MEMORANDUMS: Information receiving limited distribution because of preliminary data, security classification, or other reasons.

CONTRACTOR REPORTS: Scientific and technical information generated under a NASA contract or grant and considered an important contribution to existing knowledge.

TECHNICAL TRANSLATIONS: Information published in a foreign language considered to merit NASA distribution in English.

SPECIAL PUBLICATIONS: Information derived from or of value to NASA activities. Publications include conference proceedings, monographs, data compilations, handbooks, sourcebooks, and special bibliographies.

TECHNOLOGY UTILIZATION PUBLICATIONS: Information on technology used by NASA that may be of particular interest in commercial and other non-aerospace applications. Publications include Tech Briefs, Technology Utilization Reports and Notes, and Technology Surveys.

Details on the availability of these publications may be obtained from:

SCIENTIFIC AND TECHNICAL INFORMATION DIVISION
NATIONAL AERONAUTICS AND SPACE ADMINISTRATION
Washington, D.C. 20546